PNWD-4398

Hydrodynamic Modeling Analysis for the Fir Island Farm Restoration Project in Skagit Bay, Washington

Z Yang
T Wang

Battelle
Pacific Northwest Division
Richland, Washington 99352

Prepared for
Shannon & Wilson, Inc.
400 North 34th Street, Suite 100
Seattle, Washington 98103
under Contract No. 63526

September 2013

LEGAL NOTICE

This report was prepared by Battelle Memorial Institute (Battelle) for Shannon and Wilson as an account of sponsored research activities under Contract No. 59394/Shannon and Wilson Job # 21-1-12318.

PNWD-4398

Hydrodynamic Modeling Analysis for the Fir Island Farm Restoration Project in Skagit Bay, Washington

Z Yang
T Wang

September 2013

Prepared for
Shannon & Wilson, Inc.
400 North 34th Street, Suite 100
Seattle, Washington 98103
under Contract Number 63526

Battelle, Pacific Northwest Division
Richland, Washington 99352

Summary

Construction of dikes in estuarine and coastal systems for protection of agricultural land use over the past century has reduced the natural tidal exchange to the agriculture farm land, altered the tidal prism, and changed the sedimentation patterns in the estuarine system. To restore the tidal interaction in nearshore wetland and improve salmonid rearing habitat in Skagit Bay and estuary, the Washington Department of Fish and Wildlife is conducting the Fir Island Farm Restoration project by setting back an existing dike along the Skagit Bay front. A study of the feasibility of different restoration alternatives required detailed hydrodynamics information about pre- and post-restoration conditions at the project site.

Shannon & Wilson, Inc., the primary contractor for the restoration project, contracted Battelle Memorial Institute, Pacific Northwest Division, to provide hydrodynamic modeling analysis and consulting support for the Fir Island Farm Restoration project. The primary objective of the study was to conduct hydrodynamic modeling analysis of existing conditions, restoration alternatives, and the effects of extreme storm events on water levels and provide hydrodynamic information and recommendations about coastal processes to the Fir Island Farm Restoration project engineering design team.

The modeling approach of the project included 1) setting up a high-resolution three-dimensional hydrodynamic model of the Fir Island Farm project site based on an existing Skagit Bay Model; 2) conducting hydrodynamic model simulations for the baseline (pre-restoration) condition; 3) conducting hydrodynamic simulations for preferred restoration alternatives and comparing results with the baseline simulations, and 4) estimating the maximum water level under extreme storm events near the project site.

Model results for the restoration conditions suggest that tidal exchange between the Fir Island Farm Restoration project site and Skagit Bay can be fully restored through Claude O. Davis Slough after the removal of the bay-front dike. Some initial erosion will be expected to occur near the dike opening to the site because of high tidal velocity and bed shear stress. Within the restoration site, tidal velocity and bed shear stress will be generally small. The restoration of the tidal marsh may also slightly increase the salinities in the bay-front waters due to the increase of tidal prism at the project site. The maximum water-surface elevation due to the combined effects of an extreme high tide, the 100-year storm event, and regional sea-level rise was estimated based on model simulations, coastal engineering calculations, and a literature review. The maximum water-level projection for a 100-year return period was 4.816 m (North American Vertical Datum of 1988). This is a conservative estimate because it was assumed the 100-year maximum wind was blowing continuously in the same direction and the storm event would occur at the same time as the extreme high tide. There was also a great uncertainty (± 0.293 m) in the regional sea-level rise estimate.

Acronyms and Abbreviations

2D	two-dimensional
3D	three-dimensional
ACE	Army Coastal Engineering
cfs	cubic foot(feet) per second
ft/s	foot(feet) per second
FVCOM	Finite Volume Coastal Ocean Model
IPCC	Intergovernmental Panel on Climate Change
km	kilometer(s)
LIDAR	LIght Detection And Ranging
m	meter(s)
mm	millimeter(s)
m/s	meter(s) per second
NAVD88	North American Vertical Datum of 1988
Pa	pascal(s)
ppt	parts per thousand
USGS	United States Geological Survey
s	second(s)
SJDF	Strait of Juan de Fuca
SLR	sea-level rise
S&W	Shannon & Wilson, Inc.
WDFW	Washington Department of Fish and Wildlife
yr	year(s)

Contents

Summary iii
Acronyms and Abbreviations v
1.0 Introduction 1.1
1.1 Modeling Scope 1.1
1.2 Study Objectives and Approach 1.1
1.3 Report Contents and Organization 1.2
2.0 Model Simulation for Existing Condition 2.1
2.1 Description of Project Site 2.1
2.2 Model Description 2.1
2.3 Model Grid for the Baseline Condition 2.2
2.4 Model Results for the Baseline Condition 2.2
3.0 Hydrodynamic Modeling for Restoration Alternatives 3.1
3.1 Model Setup for Full Dike Removal Alternative 3.1
3.2 Results and Discussion for Full Dike Removal Alternative 3.1
3.3 Model Setup for the Spur Dike Alternative 3.11
3.4 Results and Discussion for Spur Dike Alternative 3.11
4.0 Estimate of Maximum Water Level 4.1
4.1 Analysis Approach 4.1
4.1.1 Estimate of Extreme Tidal Elevation (η_{tide}) 4.1
4.1.2 Estimate of 100-Year Storm Surge Height (η_{surge}) 4.1
4.1.3 Estimate of Wave Run-up (η_{wave}) 4.2
4.1.4 Long-Term Sea Level Rise (η_{slr}) 4.3
4.2 Estimate of Maximum Water Level 4.3
5.0 Conclusions 5.1
6.0 References 6.1
Acknowledgement 6.2

Figures

2.1 Study area – Skagit Bay and Fir Island Farm 2.3
2.2 Restoration project site – Fir Island Farm 2.4
2.3 Model grid of Skagit Bay and the Fir Island Farm project site 2.5
2.4 Tidal surface elevations along the model open boundaries 2.5
2.5 Skagit River flow for the period from 3/16/2003 to 4/15/2003 ..... 2.6
2.6 Wind stick at the National Oceanic and Atmospheric Administration's National Climatic Data Center weather station at the Whidbey Island Naval Base 2.6
2.7 Water-surface elevation time series comparison at Crescent Harbor station 2.6
2.8 Depth-average velocity and salinity at low tide under existing conditions 2.7
2.9 Depth-average velocity and salinity at flood tide under existing conditions 2.8
2.10 Depth-average velocity and salinity at high tide under existing conditions 2.9
2.11 Depth-average velocity and salinity at ebb tide under existing conditions 2.10
3.1 Model grids for baseline condition and full dike removal alternative 3.3
3.2 Time series of water level, depth-averaged salinity, and along-channel velocity at Station F1 in the Skagit Bay front between the baseline and full dike removal alternative 3.4
3.3 Depth-averaged salinity, along-channel velocity, and velocity scatter plot at Station F2 in the project site under the full dike removal alternative 3.5
3.4 Time series of water level, depth-averaged salinity, and velocity at Station F3 in the marsh area of the project site under the full dike removal alternative 3.6
3.5 Water depth and depth-averaged velocity at low tide near Fir Island Farm for the baseline and full dike removal alternative conditions 3.7
3.6 Water depth and depth-averaged velocity at flood tide near Fir Island Farm for the baseline and full dike removal alternative conditions 3.8
3.7 Water depth and depth-averaged velocity at high tide near Fir Island Farm for the baseline and full dike removal alternative conditions 3.9
3.8 Water depth and depth-averaged velocity at ebb tide near Fir Island Farm for the baseline and full dike removal alternative conditions 3.10
3.9 Bathymetry for the spur dike alternative and stations for model result comparisons 3.13
3.10 FVCOM model grid and bathymetry for the spur dike alternative 3.14
3.11 Time series of the water level and salinity at Station S1 in the Skagit Bay front 3.15
3.12 Time series of the depth-averaged velocity and bottom shear stress at Station S1 in the Skagit Bay front 3.16
3.13 Time series of the water level and salinity at Station S2 at the dike opening 3.17
3.14 Time series of the depth-averaged velocity and bottom shear stress at Station S2 at the dike opening 3.18
3.15 Time series of the water level and salinity at Station S3 in No Name Slough 3.19
3.16 Time series of the depth-averaged velocity and bottom shear stress at Station S3 in No Name Slough 3.20

3.17 Time series of the water level and salinity at Station S4 in the marsh area 3.21
3.18 Time series of the depth-averaged velocity and bottom shear stress at Station S4 in the marsh area 3.22
3.19 Time series of the water level and salinity at Station S5 in Claude O. Davis Slough..... 3.23
3.20 Time series of the depth-averaged velocity and bottom shear stress at Station S5 in Claude O. Davis Slough..... 3.24
3.21 Water depth and depth-averaged velocity at low tide for the baseline and spur dike alternative conditions 3.25
3.22 Water depth and depth-averaged velocity at flood tide for the baseline and spur dike alternative conditions 3.26
3.23 Water depth and depth-averaged velocity at high tide for the baseline and spur dike alternative conditions 3.27
3.24 Water depth and depth-averaged velocity at ebb tide for the baseline and spur dike alternative conditions 3.28
4.1 Wind frequency curve at NCDC station on Whidbey Island 4.4
4.2 Wind rose for the period of 1948−2013 at the NCDC station on Whidbey Island 4.5
4.3 Comparison of water-surface elevation at the bay front for the 100-year wind storm and spur dike conditions 4.6

1.0 Introduction

Population shift and land-use change over the past century have had significant impacts on the coastal ecosystem and associated marine wildlife. Construction of dikes in estuarine and coastal systems for protection of agricultural land use has reduced the natural tidal exchange to the agriculture farm land, altered the tidal prism, and changed the sedimentation patterns in the estuarine system. The changes in hydrodynamics and sedimentation in turn have resulted in reductions of the tidal channel and marsh habitat compared to historic conditions both inside and outside of dikes. One such complex and dynamic estuarine system comprises the Skagit River delta and Skagit Bay, in particular the diked-enclosed agricultural area of the delta known as Fir Island.

The Washington Department of Fish and Wildlife (WDFW) is conducting the Fir Island Farm Restoration project along Skagit Bay to restore tidal interaction and improve salmonid rearing habitat. The project involves setting back an existing dike and restoring approximately 127 acres of tidal wetland. Shannon & Wilson, Inc. (S&W) contracted Battelle Memorial Institute, Pacific Northwest Division, to provide hydrodynamic modeling analysis and consulting support for the Fir Island Estuary Restoration project.

1.1 Modeling Scope

The modeling effort consisted of four tasks: 1) hydrodynamic modeling of existing conditions in Skagit Bay and at the restoration site; 2) hydrodynamic modeling of a “full dike removal restoration” alternative; 3) hydrodynamic modeling of a “dike removal with spur dike restoration” alternative; and 4) model analysis of the effect of extreme storm events and sea-level rise on water levels near the project site. Tasks 1 and 2 were completed during a feasibility study conducted as Phase I of the project (Yang and Wang 2011; Breithaupt et al. 2011). Tasks 3 and 4 were completed during Phase II of the project (Engineering Studies and 60% Design).

1.2 Study Objectives and Approach

The primary objective of the study was to conduct hydrodynamic modeling analysis of existing conditions, restoration alternatives, and the effects of extreme storm events on water levels and provide the resulting hydrodynamic information and recommendations about coastal processes to the Fir Island Farm Restoration project engineering design team.

The general approach for modeling the dike setback alternatives and the significant wave analysis was as follows:

- Set up a three-dimensional (3D) hydrodynamic model of the Fir Island Farm Restoration project site based on the existing Skagit Bay Model developed by Battelle staff (Yang and Khangaonkar 2009).
- Conduct hydrodynamic model simulation for the baseline (pre-restoration) condition for the period selected by the project team and validate the pre-restoration hydrodynamic model using available data.

- Conduct hydrodynamic model simulations for selected preferred restoration alternatives (dike setback with and without the spur dike) using the same tidal, wind, and river inflow boundary conditions used in the baseline simulations.
- Compare the hydrodynamic responses between the pre- and post-restoration simulations.
- Conduct modeling analysis to estimate the water-surface elevations derived from the significant wave height associated with extreme tides, storm surges, and future sea-level rise conditions.

1.3 Report Contents and Organization

To present a complete restoration modeling analysis story the modeling results for Tasks 1 through 4 are included in the ensuing sections of this report. Model setup, data, model forcing inputs and model outputs including time series of water surface elevation, salinity, velocity and bed shear stress at selected locations near the project site are presented. Horizontal two-dimensional (2D) distributions of velocity vector and salinity at flood, ebb, low and high tides are also provided and discussed. In particular, Sections 2.0, 3.0, and 4.0, respectively, address the hydrodynamics for the existing baseline condition, the restoration alternatives, and the estimate of maximum water-surface elevation caused by extreme storm events. Section 5.0 provides conclusions; Section 6.0 provides references for literature cited in the narrative.

2.0 Model Simulation for Existing Condition

This section describes the overall project site and application of the Skagit Bay hydrodynamic model to simulate the tidal hydrodynamics and salinity distribution in the Skagit Bay front near the project site under existing condition.

2.1 Description of Project Site

The Skagit River is the largest river discharging to Puget Sound, and is responsible for about 34–50% of the total freshwater flow into Puget Sound. The river flow generally peaks in late spring or early summer because of snowmelt and in winter because of high precipitation. The river flow drops to the minimum in September. A significant portion of Skagit Bay is covered by a shallow-water tide flat that is exposed during low tides.

Skagit Bay connects to Puget Sound and the Strait of Juan de Fuca (SJDF) through three pathways and is subjected to strong tidal forcing. The main pathway for water exchange with Puget Sound is the Saratoga Passage of Whidbey Basin from the south, which connects to the Main Basin of Puget Sound. Deception Pass connects Skagit Bay from the east to SJDF, and the Swinomish Channel connects Skagit Bay from the north to Padilla Bay (Figure 2.1). The Skagit River enters Skagit Bay through the North Fork and the South Fork branches. The large river delta between the North Fork and South Fork is Fir Island. Fir Island has been extensively diked (leveed) for flood protection for agricultural land use. The Fir Island Farm Restoration project is located at the WDFW Snow Goose Reserve, along Skagit Bay (Figure 2.2). The project site in the existing (pre-restoration) condition is bounded by Brown Slough on the west and Dry Slough on the east, Fir Island Road on the north and bay front dike on the south. There are two drainage channels inside the project site, the No Name Slough and Claude O. Davis Slough.

Interior drainage runoff (Brown Slough, No Name Slough, and Dry Slough) in the project site is very small and was assumed to be zero in the baseline hydrodynamic modeling simulation. S&W is performing a separate interior drainage study in support of the project for hydrologic analysis. There are three tide gates located in the study area along Brown Slough, two tidegates at Dry Slough, and two tidegates at Claude O. Davis Slough. Most of the tidegates are top-hinge flap-style tidegates that discharge into the Skagit Bay.

2.2 Model Description

The hydrodynamic model used in this study is the Finite Volume Coastal Ocean Model – FVCOM (Chen et al. 2003). FVCOM is a 3D, unstructured-grid, finite volume coastal ocean model with the robust capability of simulating wetting and drying processes in the intertidal zone. FVCOM solves the 3D momentum, continuity, temperature, salinity, and density equations in an integral form for water-surface elevation and flow fields. Companion modules for sediment transport, water-quality kinetics, and biological models are also integrated into FVCOM, but were not used for this study. The model computes water depths, velocities, salinities and water-surface elevations based on the geometry and bathymetry of the system, the specified lateral and vertical boundary conditions, and model input parameters. FVCOM has been extensively applied to simulate hydrodynamics and transport processes in many locations around the world, including many restoration sites in Puget Sound.

2.3 Model Grid for the Baseline Condition

The model grid for the project site was developed based on the existing Skagit Bay hydrodynamic model (Yang and Khangaonkar 2009). A fine-grid mesh with a spatial resolution as small as 5 m was created for the project site. To further eliminate the effect of open boundary on the water circulation and freshwater plume dynamics, especially during high flow conditions, the Skagit Bay open boundary was moved farther south to Green Bank in Saratoga Passage (Figure 2.3). Model bathymetry was updated with LIght Detection And Ranging (LIDAR) data and survey data provided by WDFW and the Skagit River System Cooperative. The model consists of 20,454 nodes, 38,400 elements, and 10 uniform vertical layers. The average grid size inside the Fir Island Farm project site is about 16 m.

The model was set up for the existing condition for the period from 3/15/2003 to 4/15/2003, as requested by the project team to represent the spring juvenile Chinook migration period. Tidal elevations along the open boundaries were obtained from XTide prediction (Figure 2.4). Skagit River flow at Mt. Vernon and wind stick from 3/15/2003 to 4/15/2003 are shown in Figure 2.5 and Figure 2.6, respectively. The mean flow for the simulation period is 18,905 cfs, which is higher than the long-term mean of 15,000 cfs for March-April period, and significantly higher than the mean flow of 9,443 cfs during the initial S&W data collection period (9/1/2010 – 9/17/2010). Salinity boundary conditions were specified as 30 ppt at all the open boundaries through the water column. Salinity at the upstream river-inflow boundary was specified as zero. Initial conditions for water-surface elevation, velocity, and salinity were all set to zero.

2.4 Model Results for the Baseline Condition

The Skagit Bay and Estuary model has been calibrated in previous studies for different periods (Yang and Khangaonkar 2009). In this study, we re-validated the model performance by comparing the predicted water-surface elevation to the XTide data at Crescent Harbor station in the model domain (Figure 2.1). The comparison of model results and XTide data is shown in Figure 2.7. The good agreement between model results and XTide data indicates that the model with inclusion of Fir Island Farm is able to predict tides in Skagit Bay accurately.

Depth-average horizontal 2D velocity and salinity distributions were generated and examined in Skagit Bay at four different tidal phases. Figure 2.8 shows the depth- average salinity and velocity distribution at low tide. Significant parts of Skagit Bay were occupied by the Skagit River plume with salinity less than 5 ppt during low tide. Large areas of tide flats were shown (blank areas) in the model results and velocities in the tide flat region were very small. At flood tide, velocities in Skagit Bay increased and the freshwater plume was pushed shoreward (Figure 2.9). At high tide, brackish water only remained in a very narrow region along the bay front dikes (Figure 2.10) and velocities in the bay became small (slack before ebbing). Salinity and velocity distributions at ebb tide are shown in Figure 2.11.

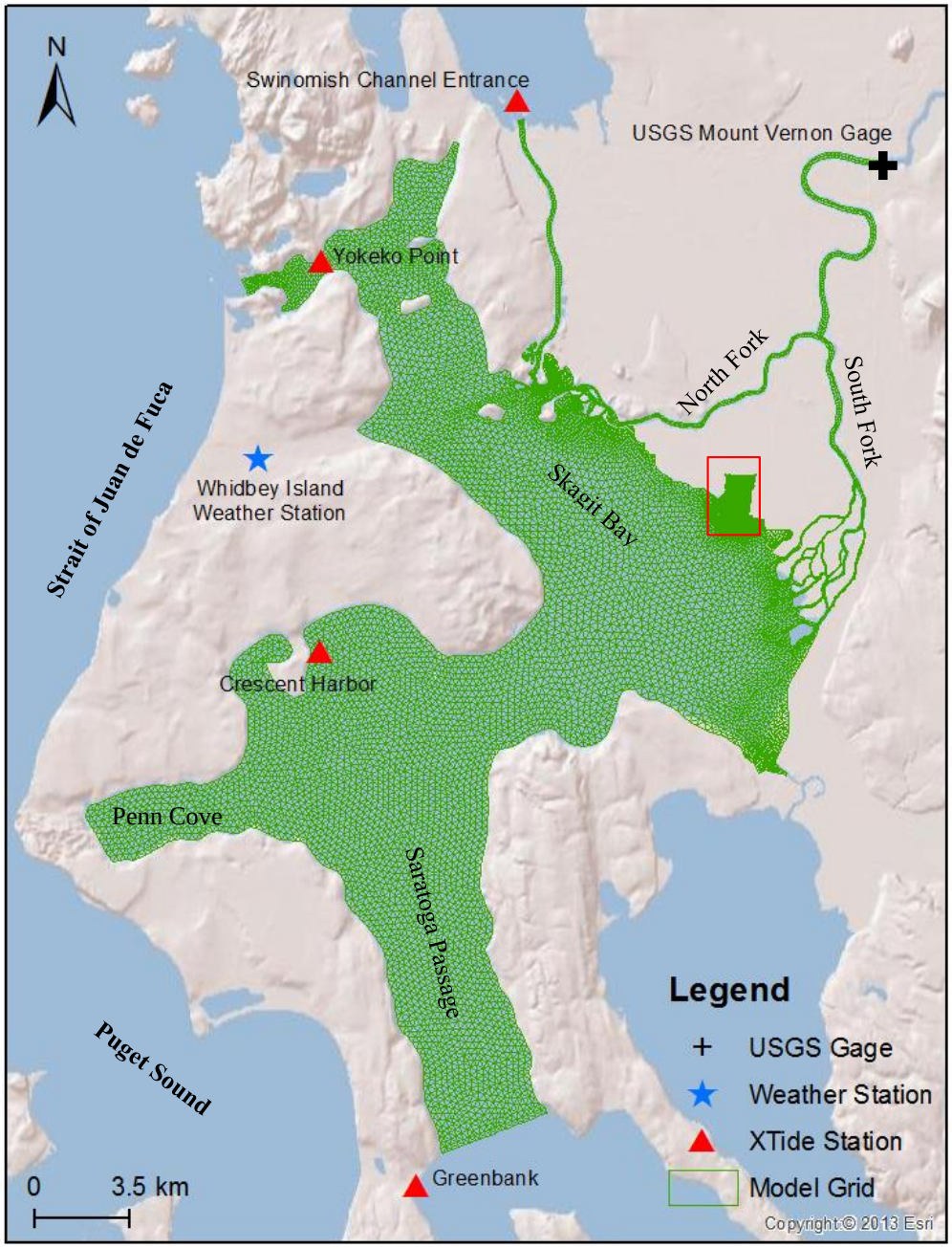

Figure 2.1. Study area – Skagit Bay and Fir Island Farm.

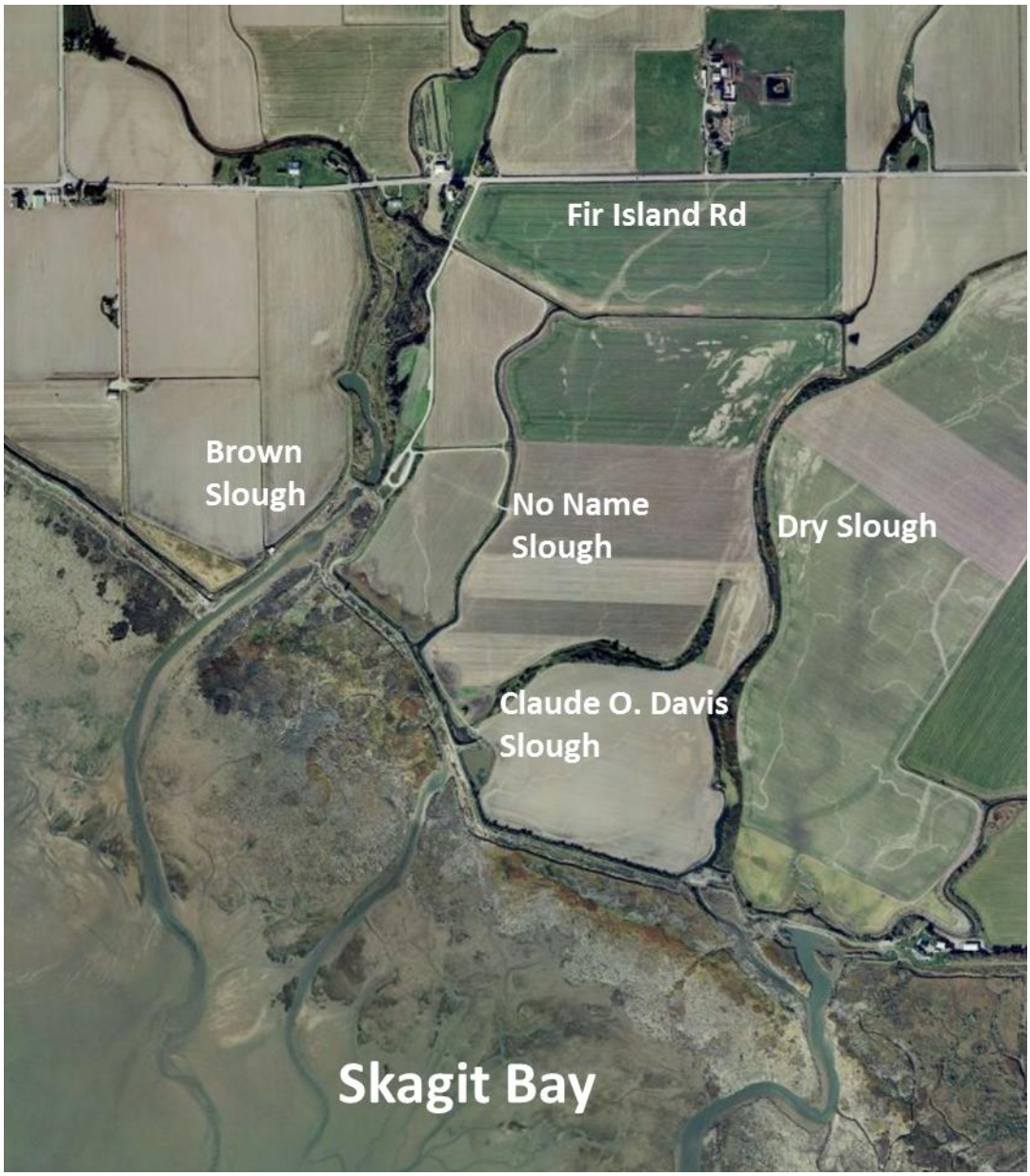

Figure 2.2. Restoration project site – Fir Island Farm.

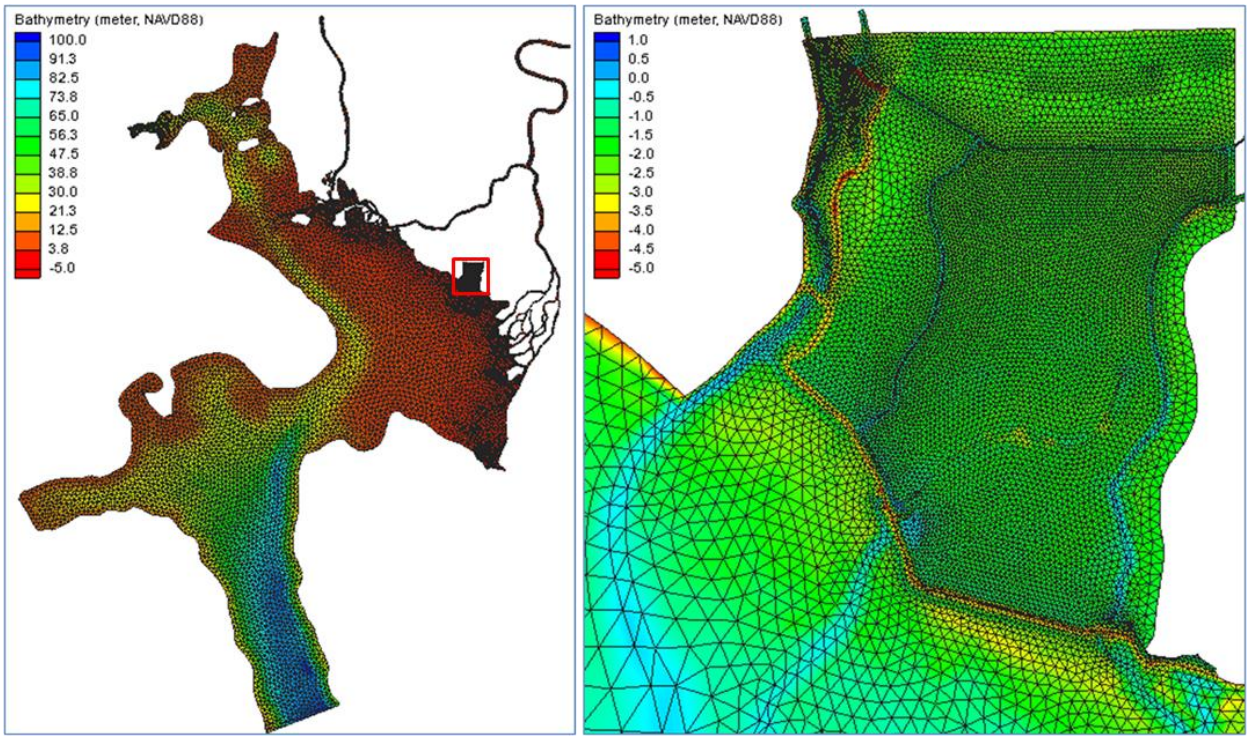

Figure 2.3. Model grid of Skagit Bay (left) and the Fir Island Farm project site (right).

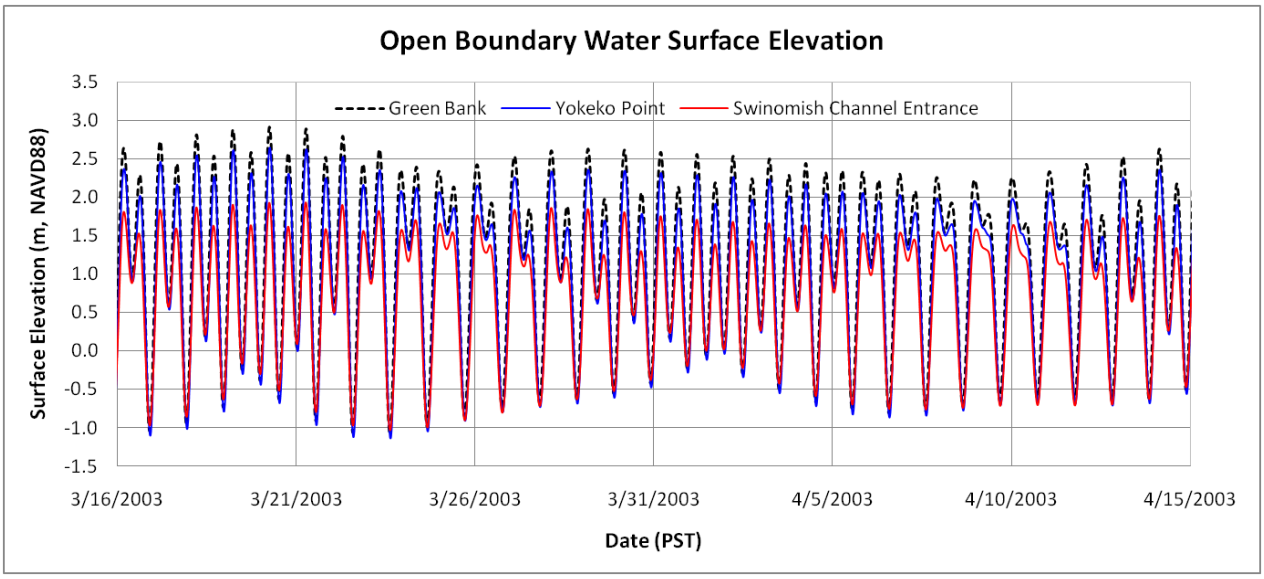

Figure 2.4. Tidal surface elevations along the model open boundaries.

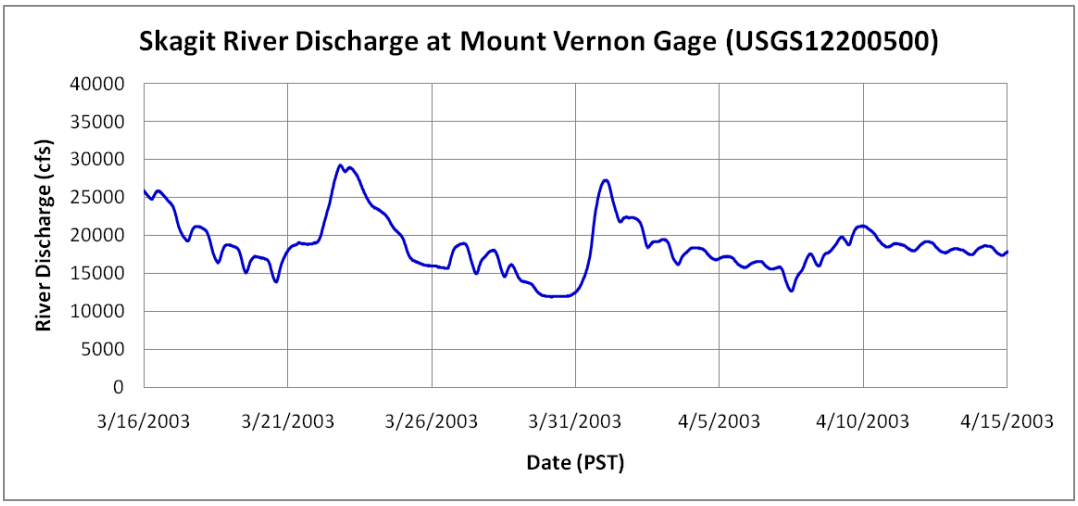

Figure 2.5. Skagit River flow for the period from 3/16/2003 to 4/15/2003.

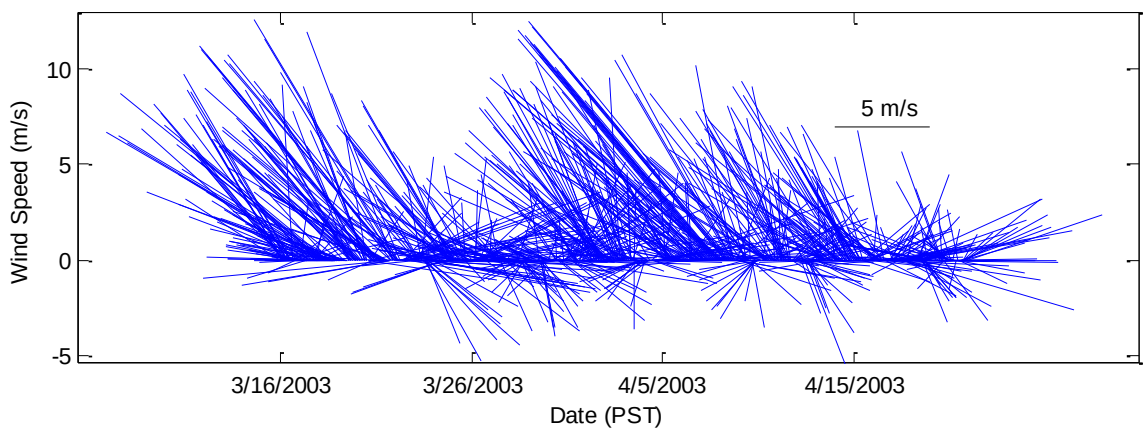

Figure 2.6. Wind stick at the National Oceanic and Atmospheric Administration's National Climatic Data Center weather station at the Whidbey Island Naval Base.

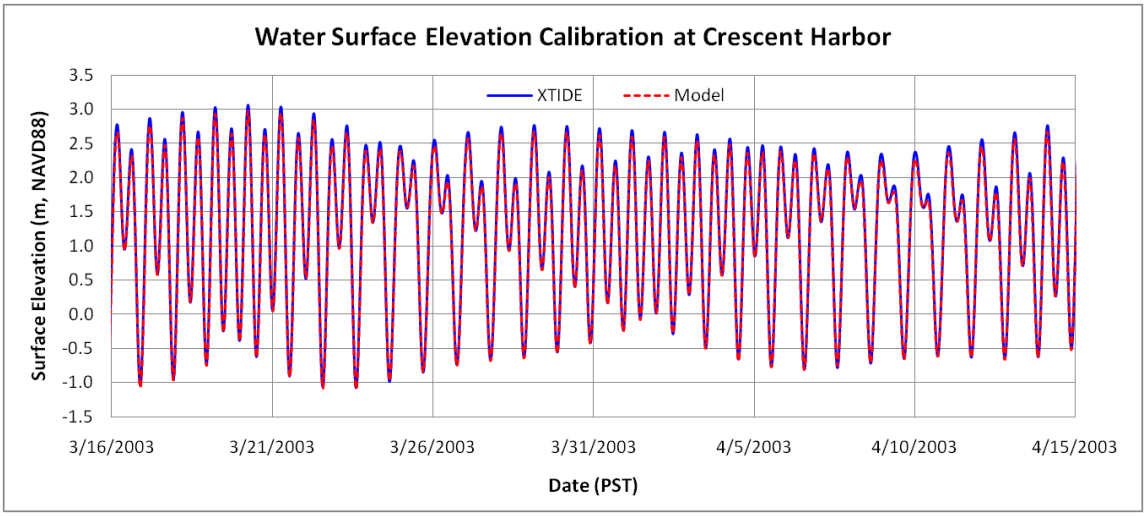

Figure 2.7. Water-surface elevation time series comparison at Crescent Harbor station.

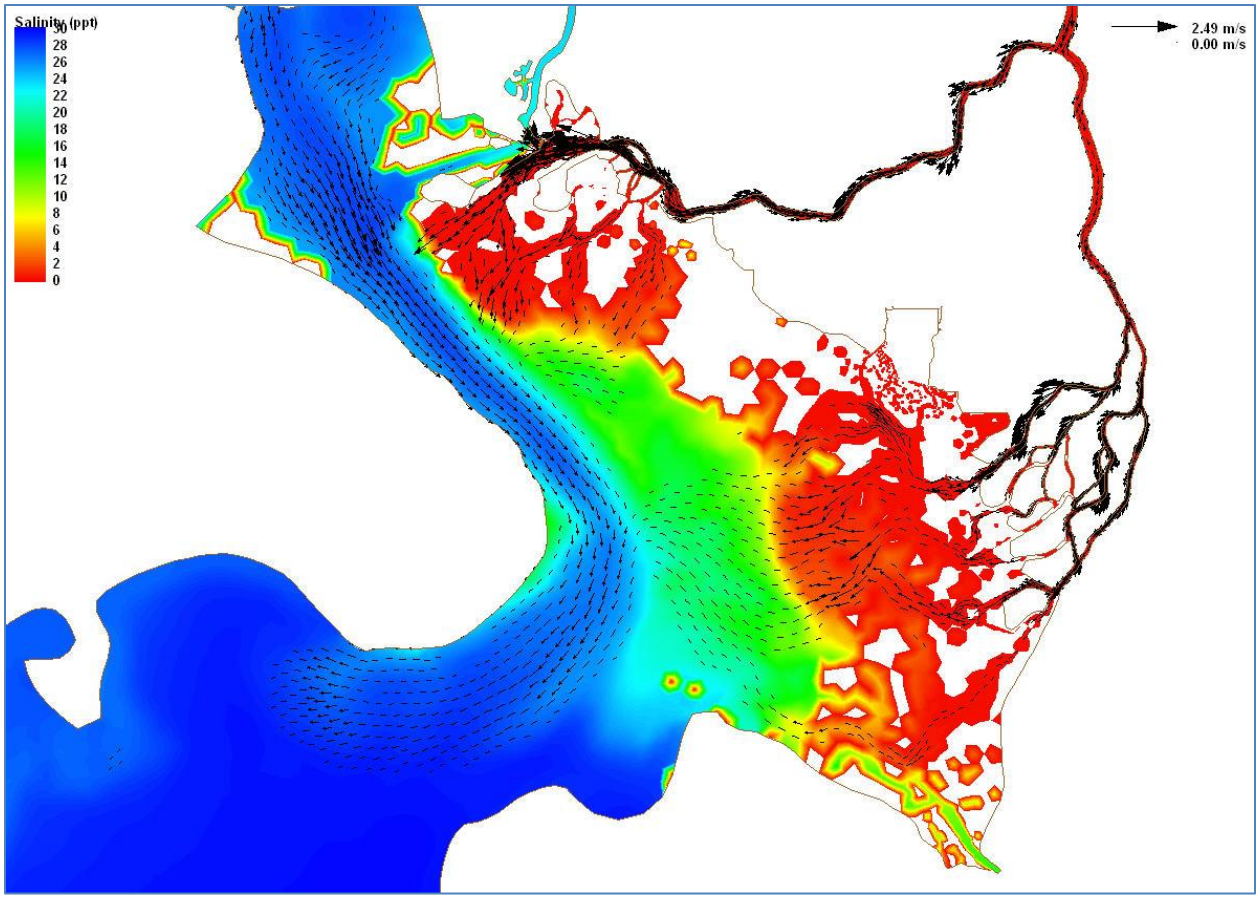

Figure 2.8. Depth-average velocity and salinity at low tide under existing conditions (4/13/2003, 8:00 p.m.)

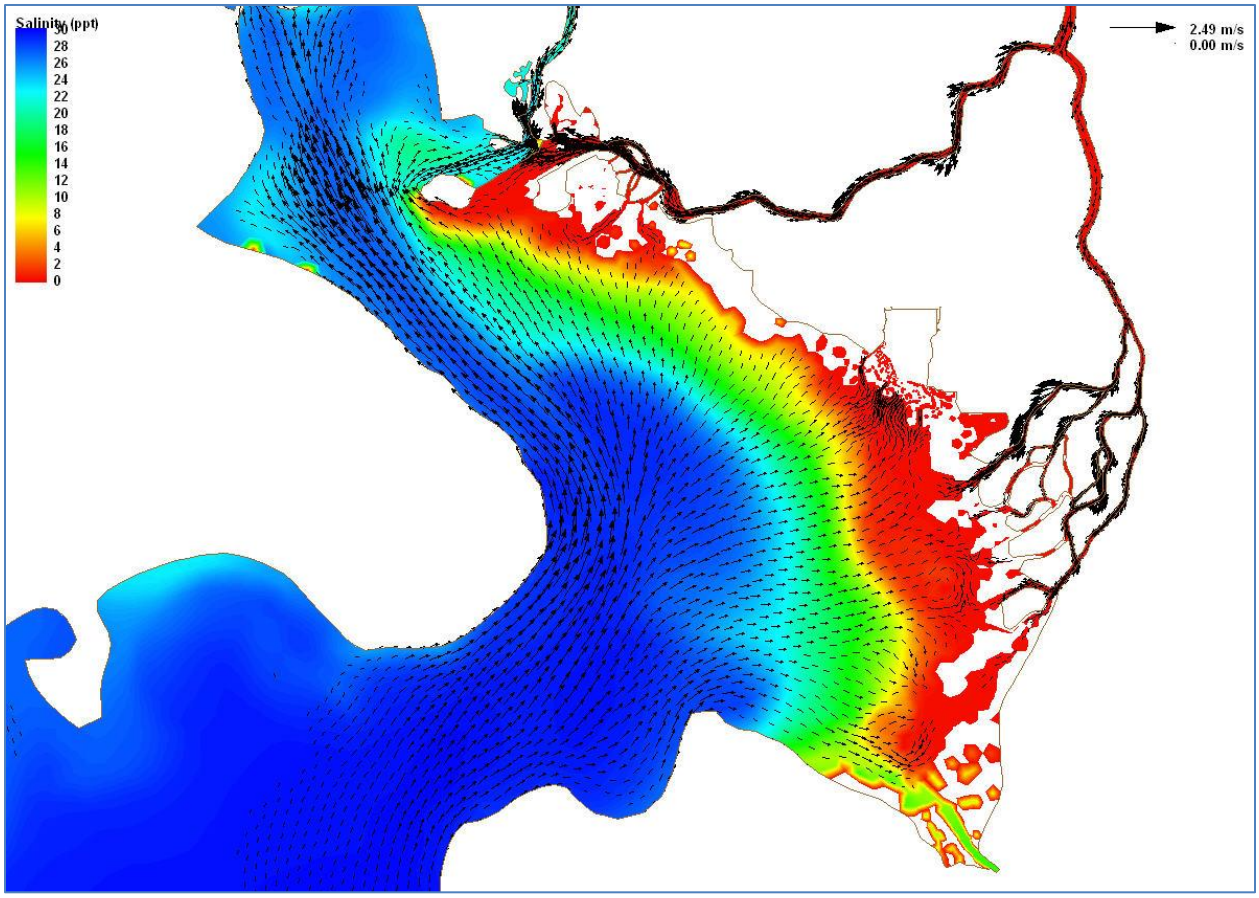

Figure 2.9. Depth-average velocity and salinity at flood tide under existing conditions (4/14/2003, 0:00 a.m.)

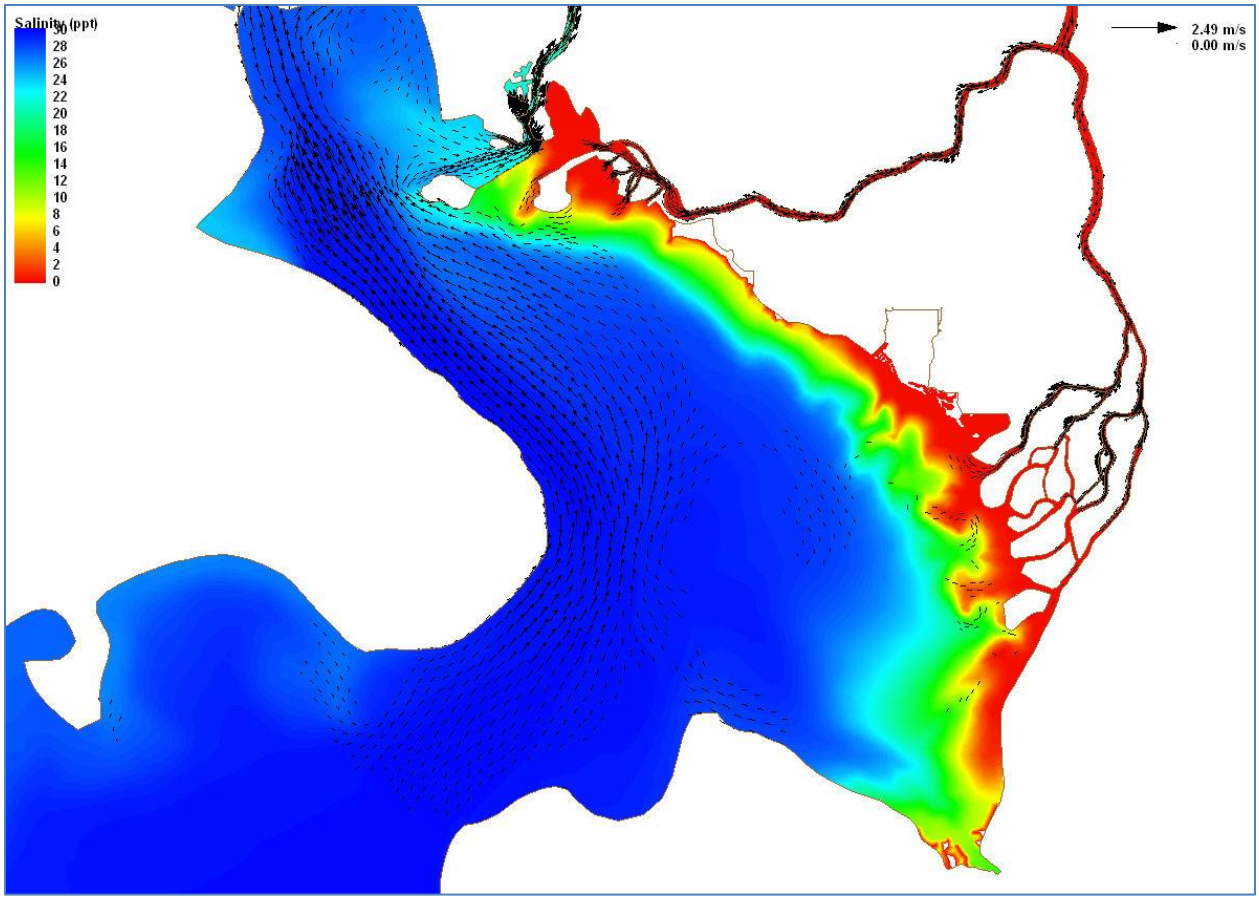

Figure 2.10. Depth-average velocity and salinity at high tide under existing conditions (4/14/2003, 3:00 a.m.)

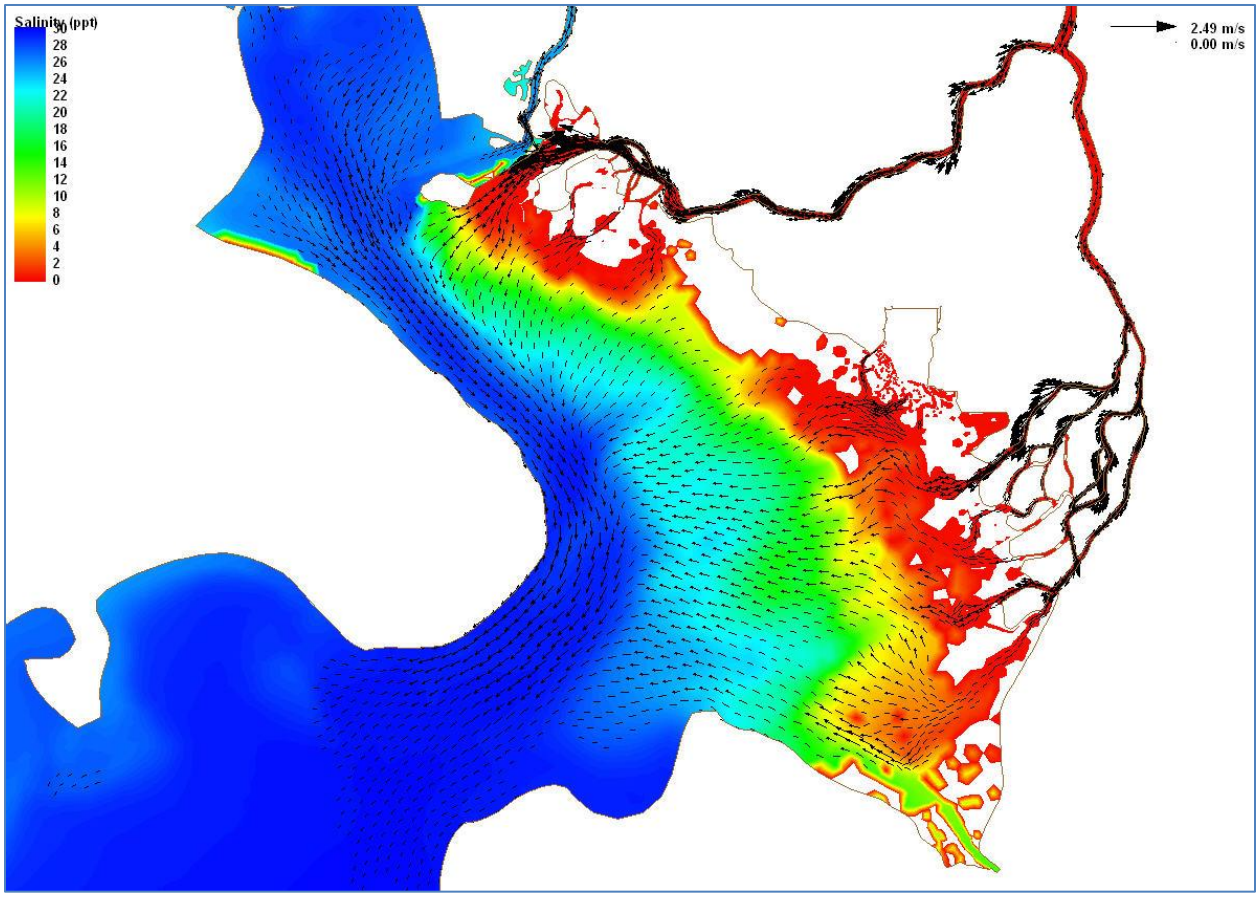

Figure 2.11. Depth-average velocity and salinity at ebb tide under existing conditions (4/14/2003, 7:00 a.m.)

3.0 Hydrodynamic Modeling for Restoration Alternatives

Upon completion of the model development for the baseline condition at the Fir Island Farm project site, the hydrodynamic model was further modified and applied to simulate the hydrodynamic conditions for the preferred restoration alternatives—the full dike removal alternative and the spur dike alternative.

3.1 Model Setup for Full Dike Removal Alternative

Model bathymetry for the full dike removal alternative was generated by modifying the baseline model bathymetry at the project site based on the alternative dike configuration provided by S&W. The full dike removal alternative involved removal of the exterior dike, placement of a new dike at the northern and eastern boundaries of the project site, addition of small "starter" channels within the project site, and deepening of the existing interior drainage channels of No Name and Claude O. Davis Sloughs. Comparison of the model grids between the baseline condition and the full dike removal alternative is shown in Figure 3.1.

The model setup for the full dike removal alternative covered the same analysis period, from 3/15/2003 to 4/15/2003, as that used for the baseline condition. The boundary conditions for tidal forcing, wind, and Skagit River flow were same specified for use in the baseline condition.

3.2 Results and Discussion for Full Dike Removal Alternative

Figure 3.2 provides the comparisons of water-surface elevation, salinity, and velocity time series between the baseline and full dike removal alternatives at a bay front location near the project site (F1 in Figure 3.1) over a spring-neap tidal cycle. The time series shows the effect of the tide flats on water-surface elevations at low tide, with no difference between the baseline and full dike removal alternative conditions. Depth-averaged salinities at the same location showed large temporal variations over each tidal period, peaking up to 14 ppt during high tides and dropping down to zero during low tides (Figure 3.2). There are no significant differences in salinity response between the existing and alternative conditions. There was little salinity stratification over the simulation period because of the shallow water depth near the project site. Velocities at F1 were small, generally within 0.2 m/s (0.6 ft/s) and dominated by flood currents. Velocities during ebb and low tides were basically zero because the grid cell became dry as the tidal elevation dropped to the ground elevation of the grid cell. There was little difference between the depth-averaged velocities of the existing and alternative conditions; hence, we expect no significant change in sediment transport characteristics in the bay front area near this location.

Figure 3.3 shows the depth-averaged salinity and along-channel velocity time series and velocity scatter plot at Station F2 in the channel of Claude O. Davis Slough inside the project site under the full dike removal alternative. The salinity at Station F2 is very low (<2 ppt) throughout the entire simulation period. The velocity scatter plot (u and v components refer to east and north velocities, respectively) shows the alignment of velocity direction with the channel orientation. In general, velocities during flood tide (positive) are below 0.2 m/s. Velocities during ebb tide are small most of the time, but occasional high ebb velocities over 0.4 m/s are observed.

Figure 3.4 shows the depth-averaged salinity and along-channel velocity time series and velocity scatter plot at Station F3 in the marsh area. Salinity at F3 is similar to that in the tidal channel (Figure 3.3). At slack high tide or low tide, velocities are close to zero. During flooding or ebbing, velocities tend to spike as tidal exchange forces Skagit Bay water through the project site. Velocity distribution in the marsh area has widely varying directions as water inundates or retreats from the marsh area, as indicated by the scatter plot (Figure 3.4).

Depth-averaged 2D velocity and water-depth distributions are shown in Figure 3.5 through Figure 3.8 for the project site during four different tidal phases. Figure 3.5 shows that during low tide most of the site is dry (<0.1 m or 0.33 ft) and the project site is draining out via Claude O. Davis Slough. When Skagit Bay begins to flood (Figure 3.6), the project site is inundated by water flowing from Claude O. Davis Slough and Brown Slough. Strong velocities (>1 m/s or 3.3 ft/s) are seen at the channel openings to the site. At high tide (Figure 3.7), the project site is fully inundated and velocities are small (<0.02 m/s or 0.06 ft/s). Similar to flood tide, drainage from the project site occurs via Claude O. Davis Slough and Brown Slough during ebb tide and strong velocities are seen near the mouths of the channels (Figure 3.8). Based on the velocity distribution under the full dike removal alternative, the channel mouths may expect some initial erosion when the Fir Island Farm project is restored and will become stabilized when the channels reach dynamic equilibrium.

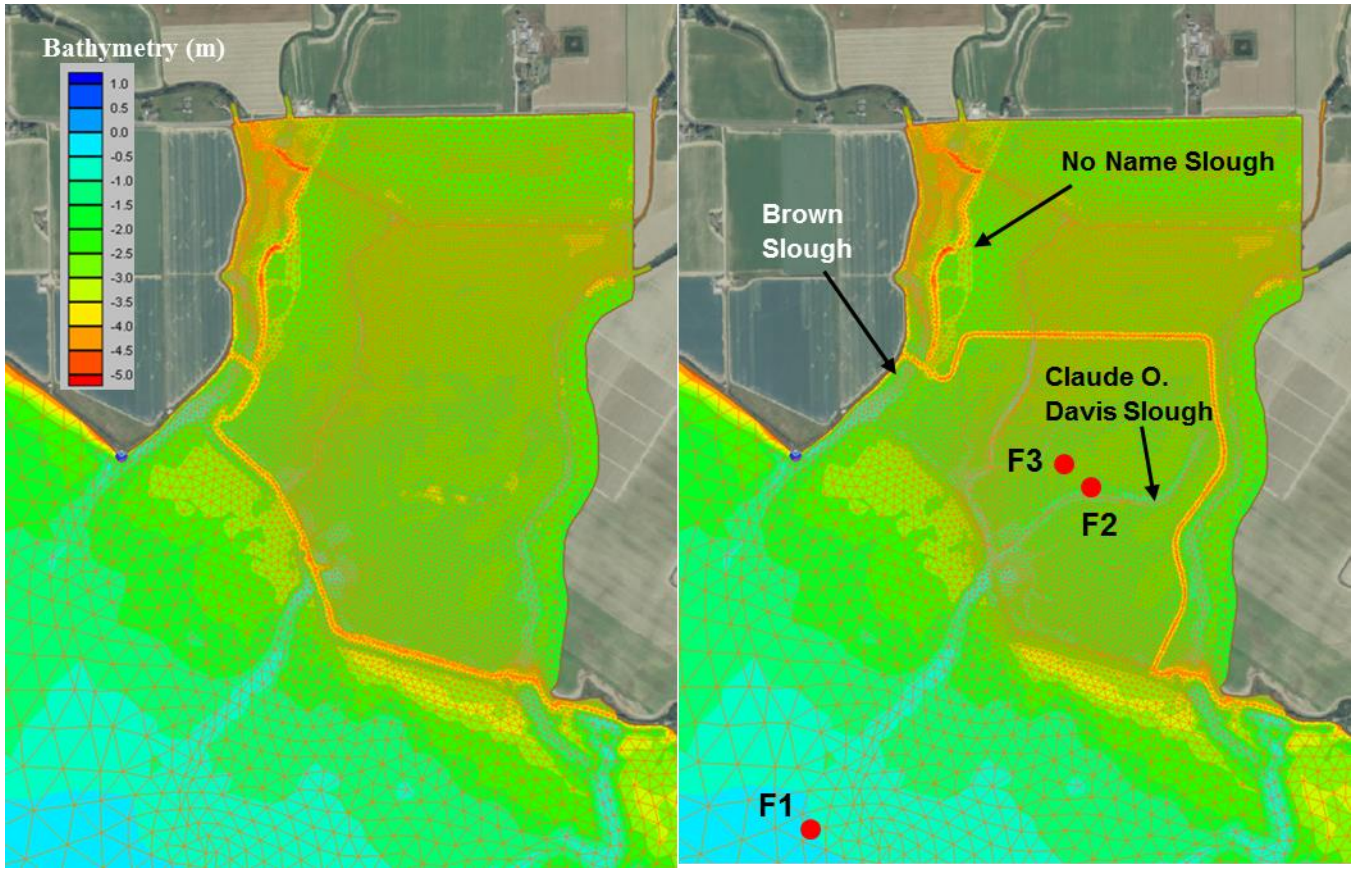

Figure 3.1. Model grids for baseline condition (left) and full dike removal alternative (right). Red circles denote station locations for model result comparisons.

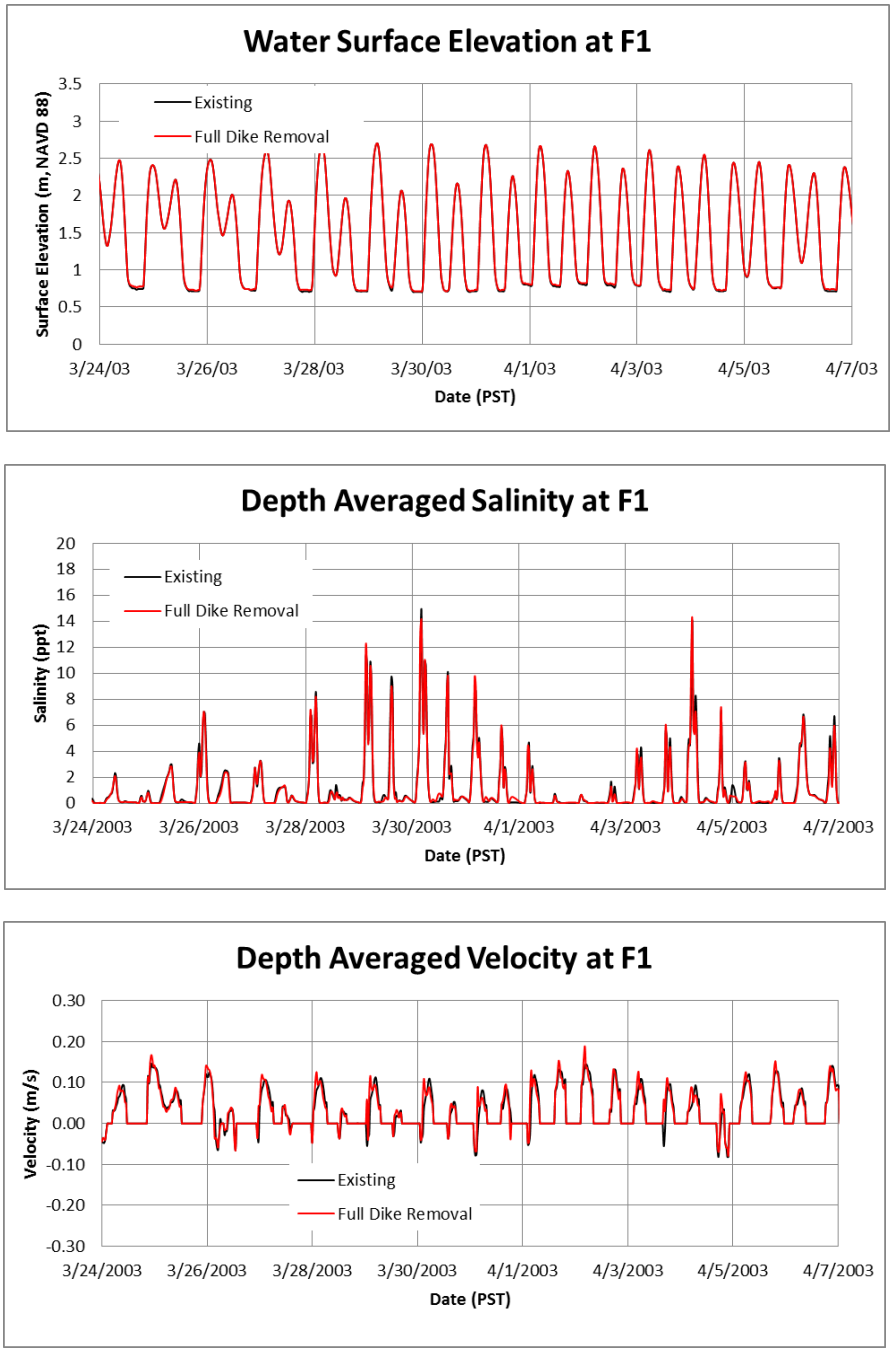

Figure 3.2. Time series of water level, depth-averaged salinity, and along-channel velocity at Station F1 in the Skagit Bay front between the baseline and full dike removal alternative.

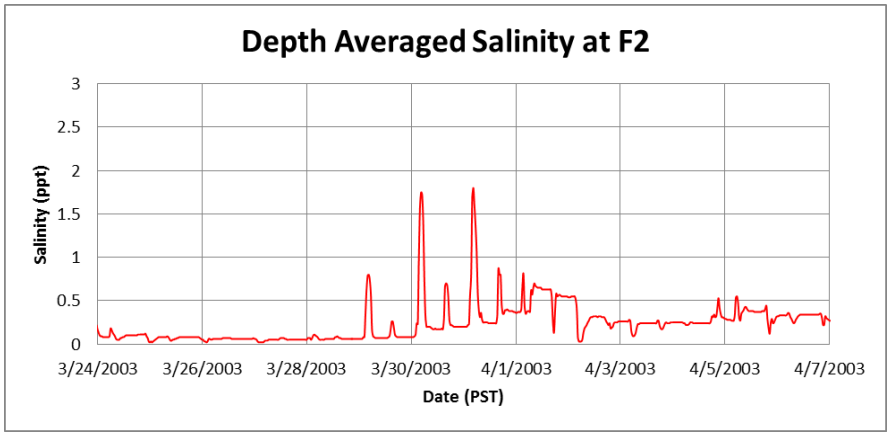

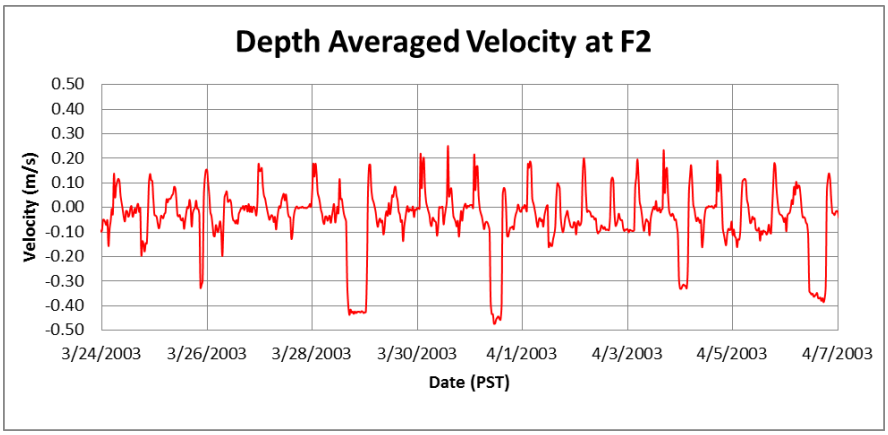

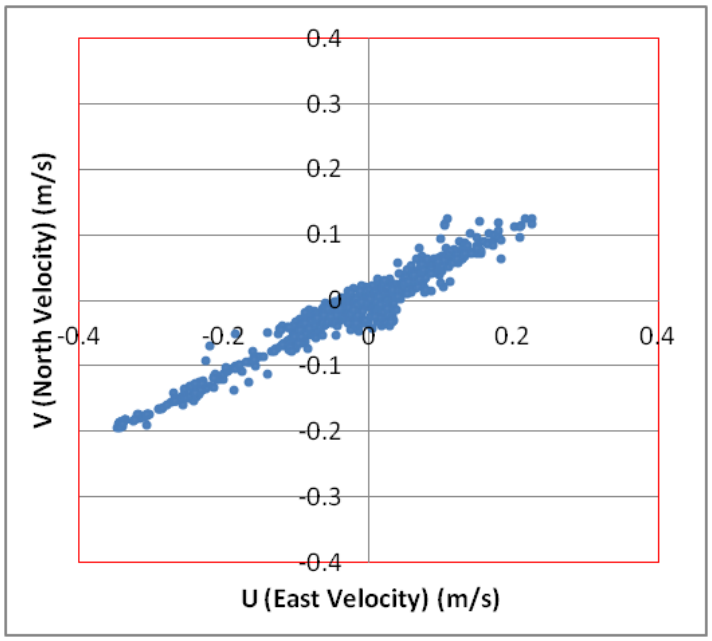

Figure 3.3. Depth-averaged salinity, along-channel velocity, and velocity scatter plot at Station F2 in the project site under the full dike removal alternative. Positive velocity denotes flooding.

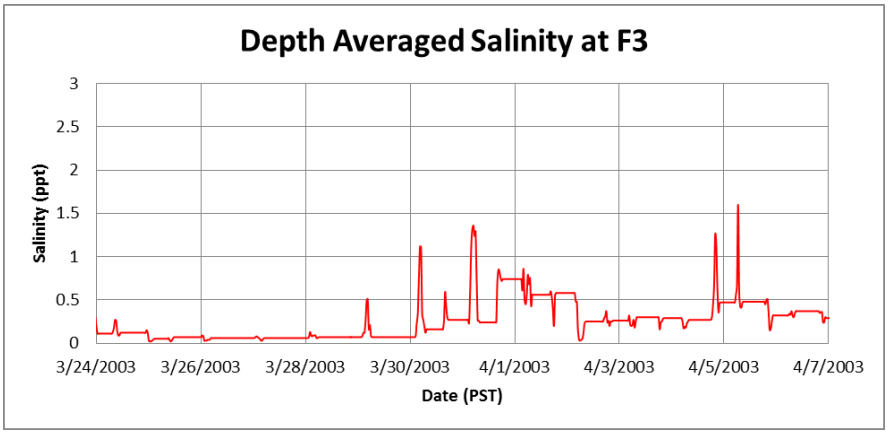

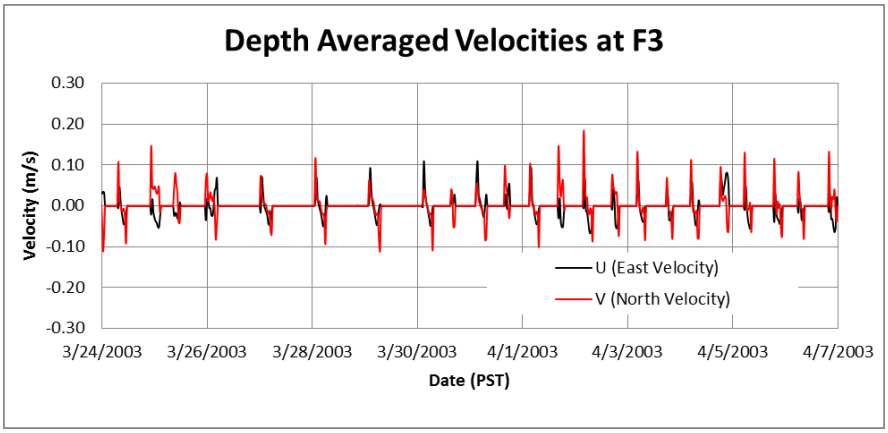

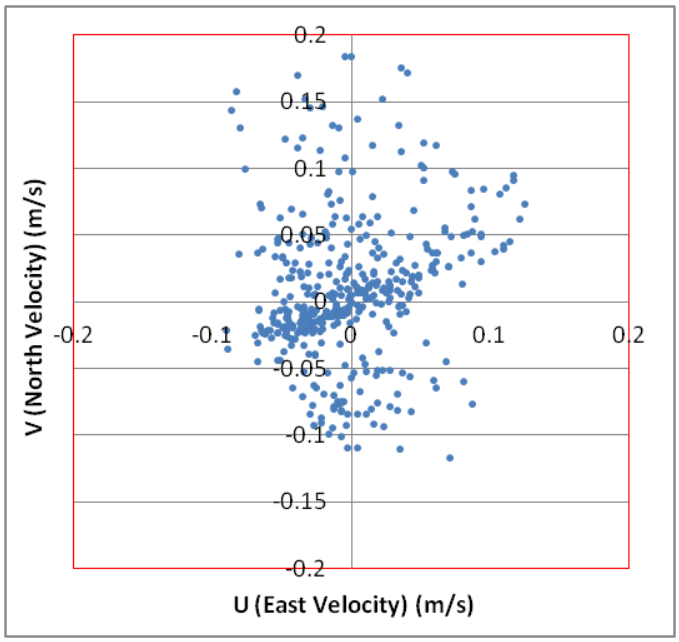

Figure 3.4. Time series of water level, depth-averaged salinity, and velocity at Station F3 in the marsh area of the project site under the full dike removal alternative.

Baseline Condition

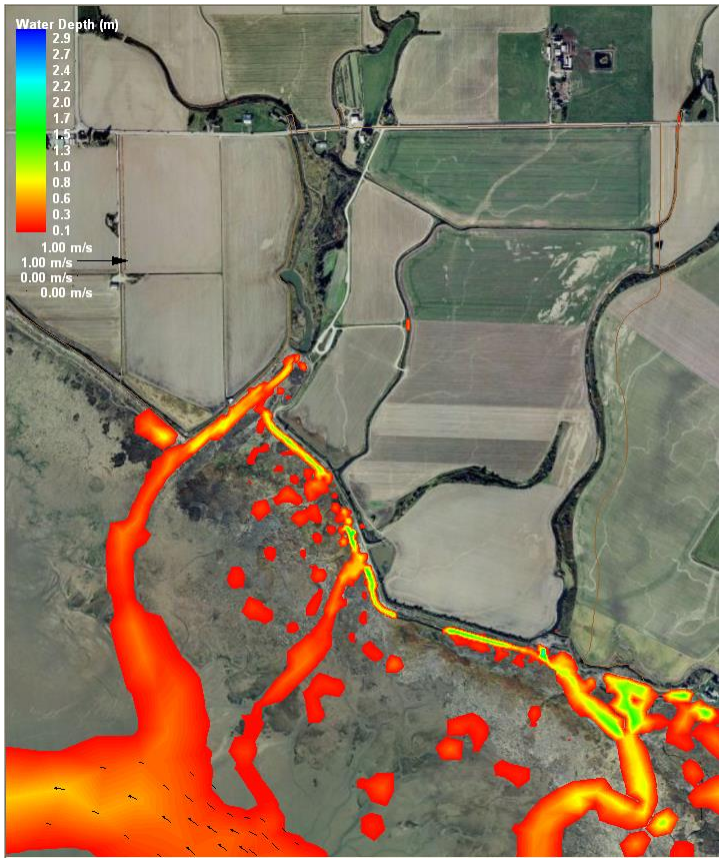

Full Dike Removal Alternative

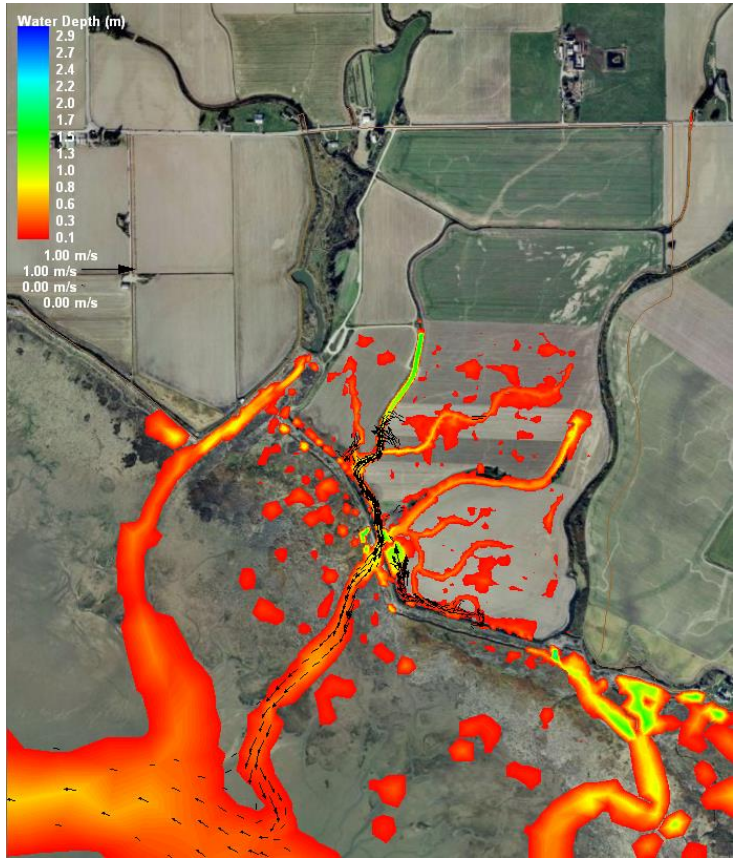

Figure 3.5. Water depth and depth-averaged velocity at low tide near Fir Island Farm (4/13/2003, 8:00 p.m.) for the baseline and full dike removal alternative conditions.

Baseline Condition

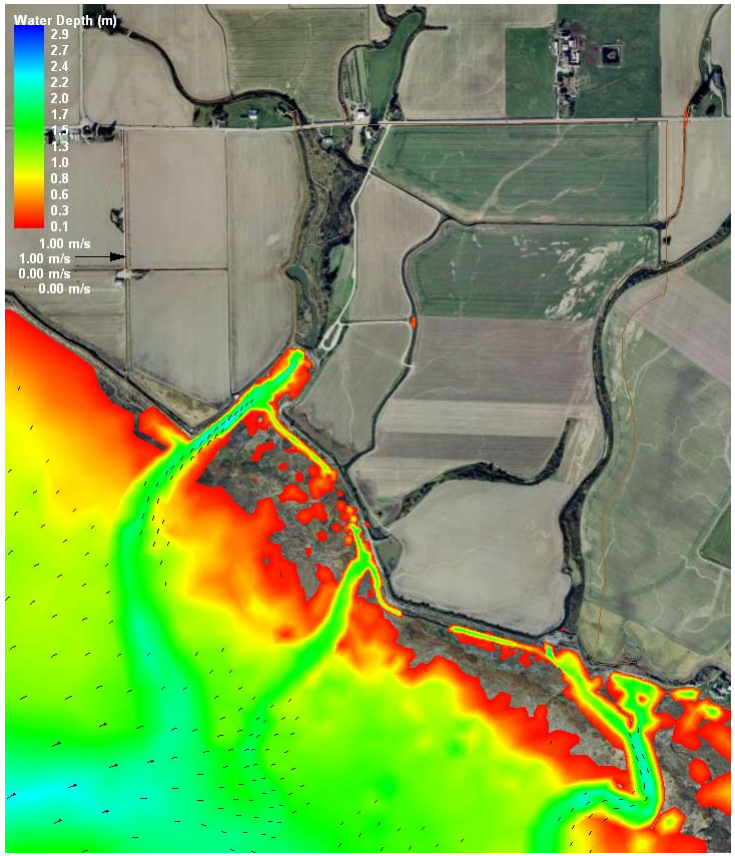

Full Dike Removal Alternative

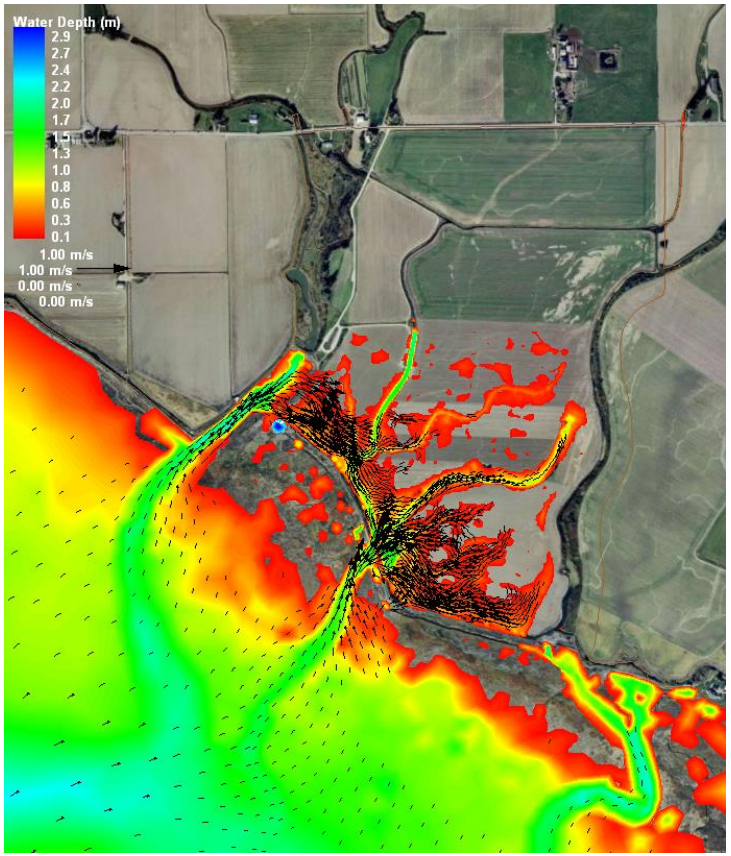

Figure 3.6. Water depth and depth-averaged velocity at flood tide near Fir Island Farm (4/14/2003, 1:30 a.m.) for the baseline and full dike removal alternative conditions.

Baseline Condition

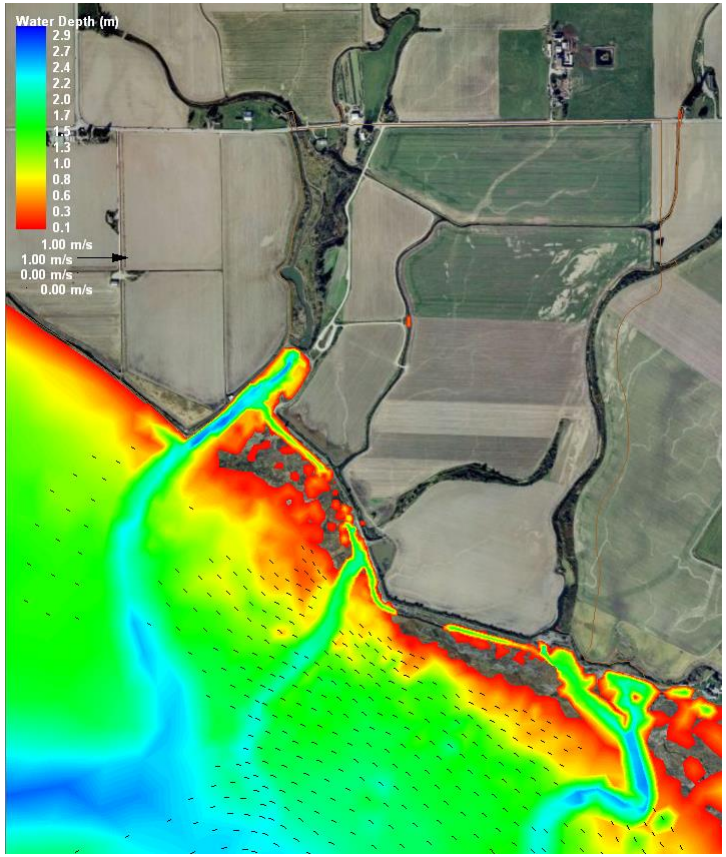

Full Dike Removal Alternative

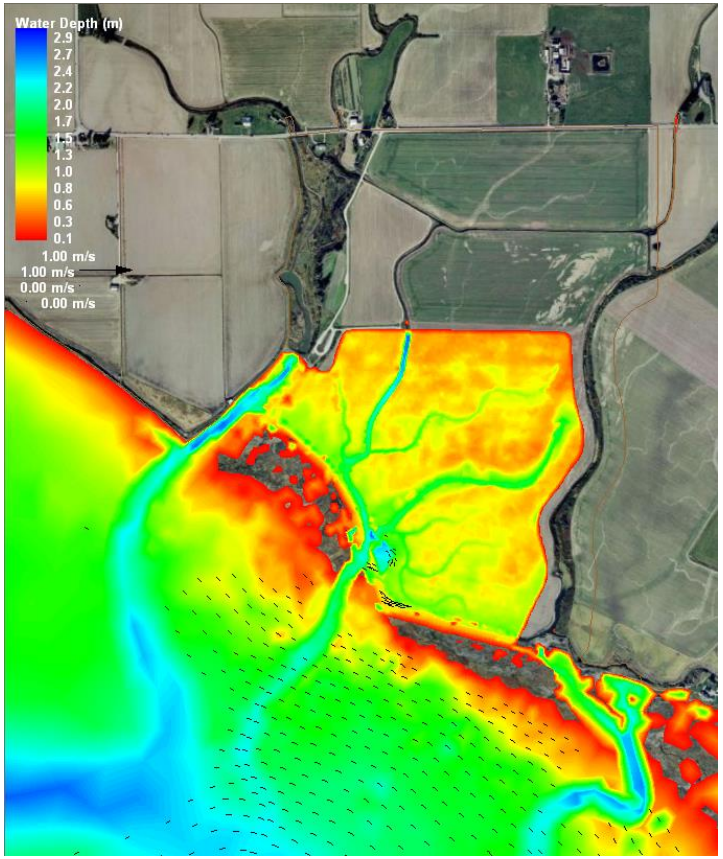

Figure 3.7. Water depth and depth-averaged velocity at high tide near Fir Island Farm (4/14/2003, 3:00 a.m.) for the baseline and full dike removal alternative conditions.

Baseline Condition

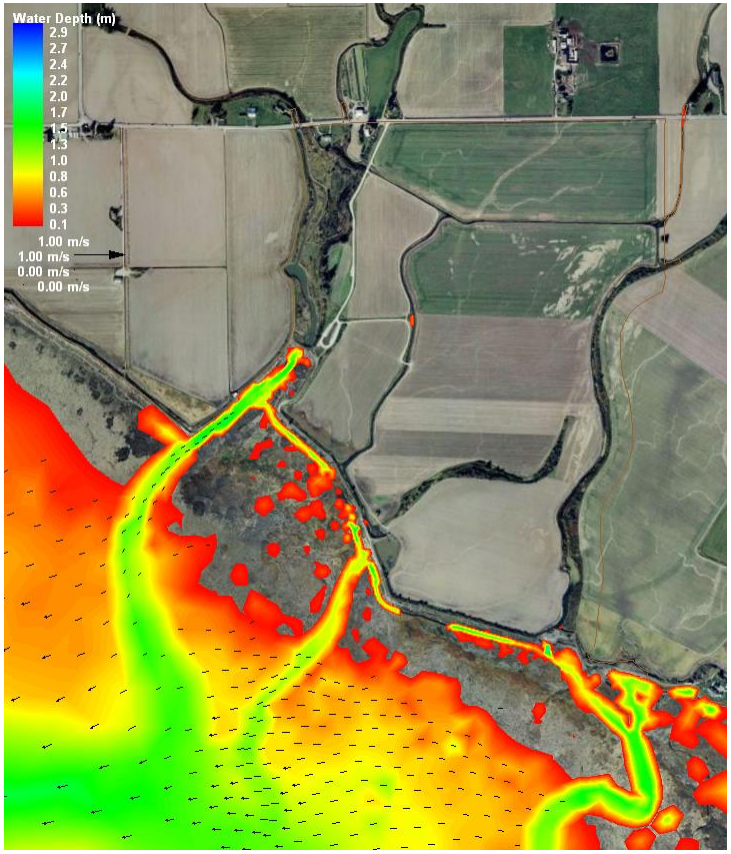

Full Dike Removal Alternative

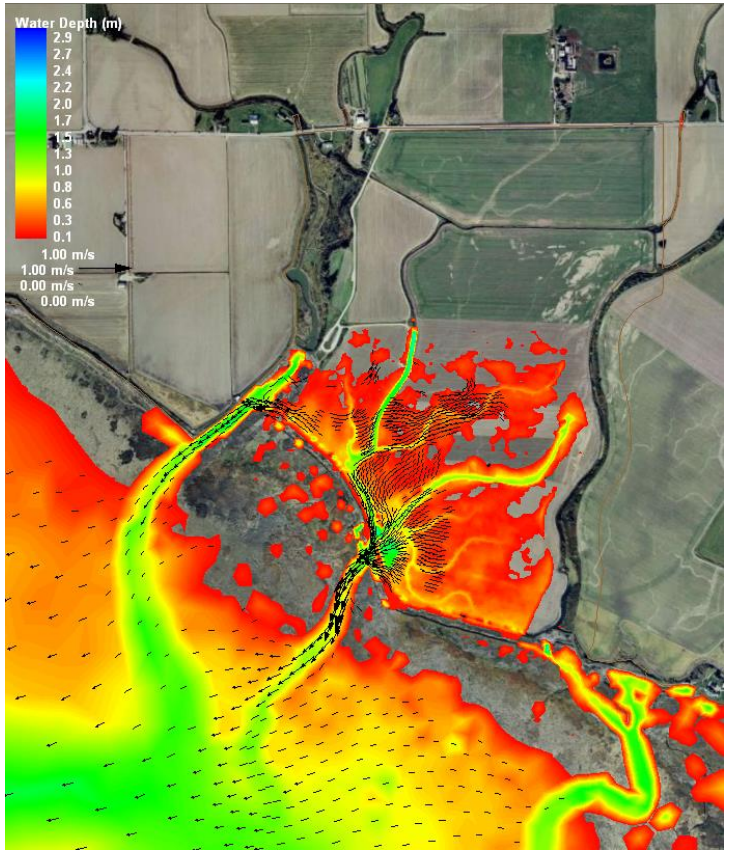

Figure 3.8. Water depth and depth-averaged velocity at ebb tide near Fir Island Farm (4/14/2003, 6:00 a.m.) for the baseline and full dike removal alternative conditions.

3.3 Model Setup for the Spur Dike Alternative

The objective of the modeling analysis for the spur dike alternative is to evaluate the hydrodynamic effects of using a spur dike to limit hydrodynamic effects on Brown Slough. The spur dike alternative involved removal of the exterior dike to the end of the public access trail on the western section of the existing dike, extension of the spur dike across the adjacent tidal channel to limit tidal inflow and outflow from this location, placement of a new dike at the northern and eastern boundaries of the project site, addition of small drainage channels within the project site, and deepening of the existing interior drainage channels of No Name and Claude O. Davis Sloughs. Model grid and bathymetry for the spur dike restoration alternative was modified at the project site based on the grading plan provided by S&W (Figure 3.9). The new model grid for the spur dike alternative consists of 23,840 nodes and 45,171 elements. To resolve the small features in the restored condition, such as the change of in-channel bathymetry in the project site, the model grid resolution was further refined to as small as 5 m (Figure 3.10). The model setup for the spur dike alternative covered the same analysis period, from 3/15/2003 to 4/15/2003, as that used for the baseline condition. The boundary conditions for tidal forcing, surface wind, and Skagit River flow were also kept the same as those used for the baseline condition.

3.4 Results and Discussion for Spur Dike Alternative

Figure 3.11 provide the time series of water-surface elevation and salinity at a bay front location near the project site (S1 in Figure 3.9) for a spring-neap tidal cycle. The time series shows the effect of the tide flats on water-surface elevations at low tide, showing no difference between baseline and spur dike restoration conditions at high tide (Figure 3.11). At low tide, water-surface elevations for the spur dike alternative are slightly higher than the baseline condition, presumably due to the ebbing flow from the restored project site. Depth-averaged salinities at the same location showed large temporal variations over each tidal cycle, peaking up to 12 ppt during high tides and dropping down to zero during low tides (Figure 3.11). The salinity for the spur dike alternative was noted to be generally higher than the baseline condition due to more tidal water intrusion into the restoration site following the dike removal. There was little salinity stratification over the simulation period because of the shallow water depths.

Figure 3.12 shows the time series of velocity and bed shear stress at Station S1 over a spring-neap tidal cycle. The depth-averaged velocities at Station S1 are respectively plotted in the East-West and North-South directions. The spur dike alternative shows much stronger ebbing flow than the baseline condition, with the North-South velocity peaking up to -0.4 m/s (negative velocity denotes ebbing). The duration of ebbing flow in the spur dike alternative is also much longer than that in the baseline condition. The bed shear stress in the spur dike alternative shows response similar to those for the depth-averaged velocities; higher shear stress and a longer duration of shear are caused by the intensified ebbing flow.

Figure 3.13 shows the time series of water-surface elevation and salinity at Station S2 located in the tidal channel of the Claude O. Davis Slough during a spring-neap tidal cycle for the spur dike alternative. As expected, the tidal range is reduced compared with Station S1 due to Station S2's higher ground elevation and sustaining tidal flow. S2 depth-averaged salinity values drop to less than 7 ppt compared with S1 and show large temporal variations over each tidal cycle (Figure 3.13). Compared with S1, depth-averaged velocities at S2 are much intensified; velocity magnitude in both directions peaks up to 1 m/s (Figure 3.14). In general, the velocity magnitude is larger at flood than ebb, but the duration of the ebbing flow is longer than the flooding flow (Figure 3.14). Bed shear stress is greatly increased at S2

because of stronger tidal currents, and the maximum values exceed 15 Pa (Figure 3.14). As a result of high bed shear stress, sediment erosion could occur at S2, which is located at the opening of the dike.

Figure 3.15 shows the time series of water-surface elevation and depth-averaged salinity at Station S3, which is located in the channel of No Name Slough at the restoration site. Both water-surface elevation and salinity show smaller temporal variations compared with Station S2 because of Station S3's higher ground elevation and location farther away from the Skagit Bay. Depth-averaged velocities are weak and generally on the order of 0.1 m/s in both flooding and ebbing directions (Figure 3.16). As a result, bed shear stress is also very small, suggesting a low potential for sediment erosion (Figure 3.16).

Figure 3.17 shows the time series of water-surface elevation and depth-averaged salinity at Station S4, which is located in the marsh area of the restoration site. It can be seen that both water-surface elevation and salinity show even smaller temporal variations than those that at Station S3. The depth-averaged tidal velocities and bed shear stress are similar to Station S3 but with smaller magnitudes (Figure 3.18), suggesting even lower potential for sediment erosion.

Figure 3.19 shows the time series of water-surface elevation and depth-averaged salinity at Station S5, which is located in the channel of Claude O. Davis Slough at the restoration site. The tidal range and depth-averaged salinity are very small. The depth-averaged velocities at S5 are higher than Stations S3 and S4, but the magnitudes in both flooding and ebbing directions are generally less than 0.2 m/s (Figure 3.20). The bed shear stress is slightly increased at S5 compared with those at S3 and S4, but generally below 0.4 Pa. Thus, the sediment erosion potential at S5 is also low (Figure 3.20).

Figure 3.21 through Figure 3.24 show the depth-averaged 2D velocity and water-depth distributions in the restoration site for the spur dike alternative during four different tidal phases. Figure 3.21 shows that during low tide most of the project site becomes dry (water depth <0.1 m) and water drains out from the restoration site via Claude O. Davis Slough. When Skagit Bay begins to flood (Figure 3.22), the project site is primarily flooding from Claude O. Davis Slough. Strong velocities (>1 m/s) are seen at the channel openings to the project site. At high tide (Figure 3.23), the project site is fully inundated and velocities are generally very small (<0.03 m/s) in most parts of the restoration site. Similar to flood tide, drainage from the project site occurs primarily via Claude O. Davis Slough during ebb tide and strong velocities are seen near the mouths of the channels (Figure 3.24). Based on the velocity distributions and the shear stress time series in Figure 3.14, the channel mouths may expect some initial erosion when the project site is restored and will become stabilized when the channels reach dynamic equilibrium. Based on the 2D plots, it is expected that the spur dike constructed to the east of Brown Slough would effectively block the tidal exchange between Brown Slough and the restoration site.

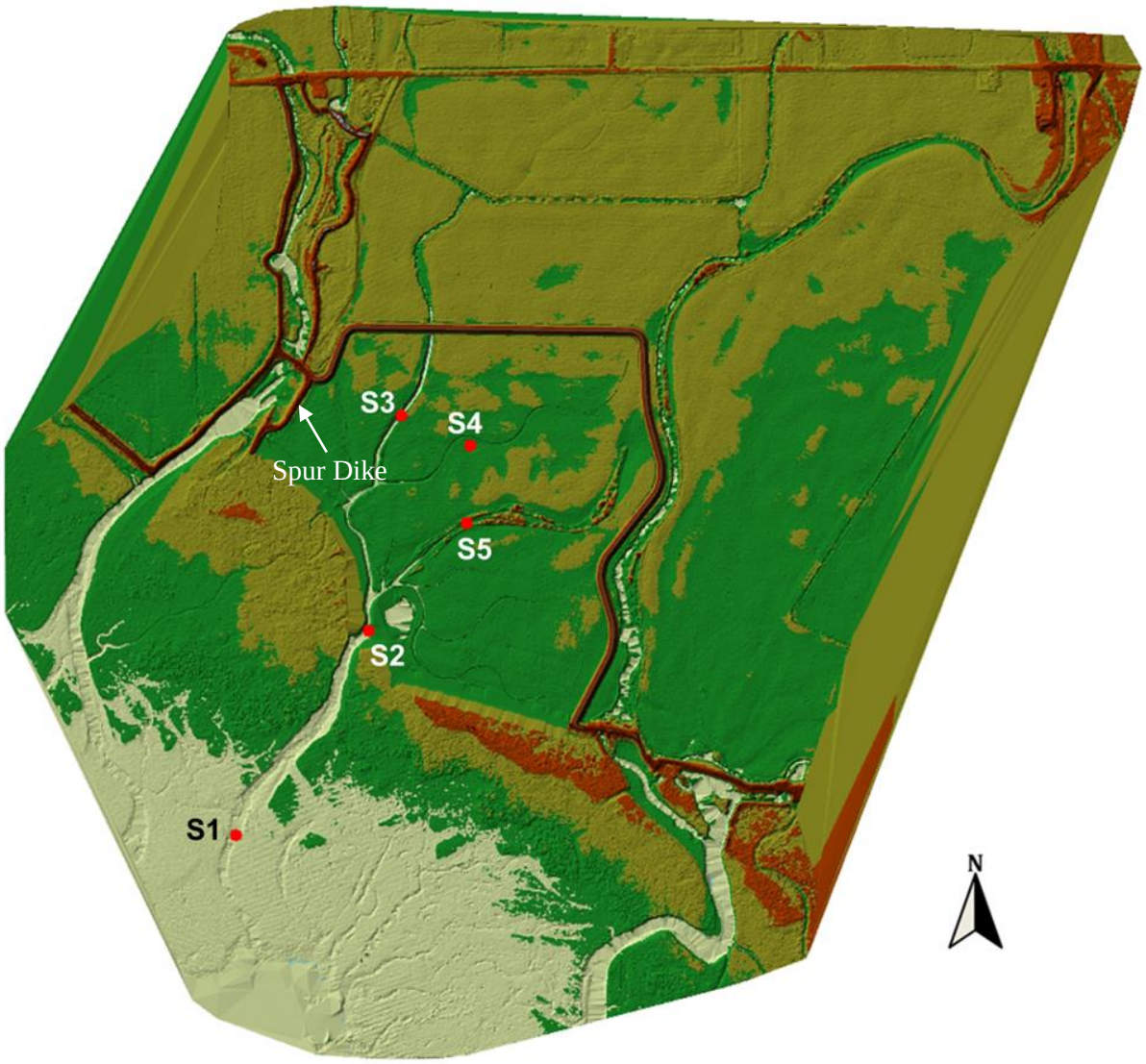

Figure 3.9. Bathymetry for the spur dike alternative and stations for model result comparisons.

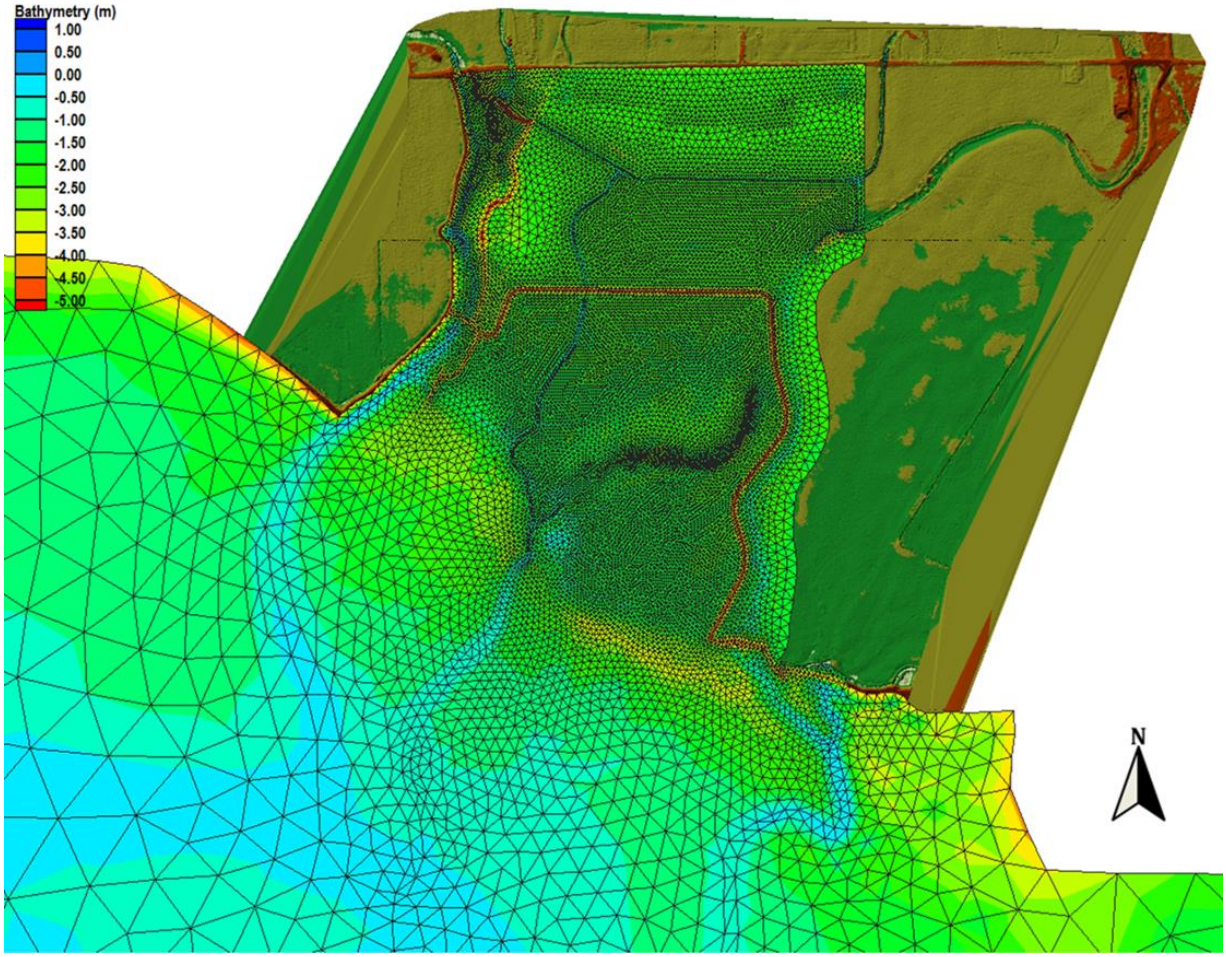

Figure 3.10. FVCOM model grid and bathymetry for the spur dike alternative.

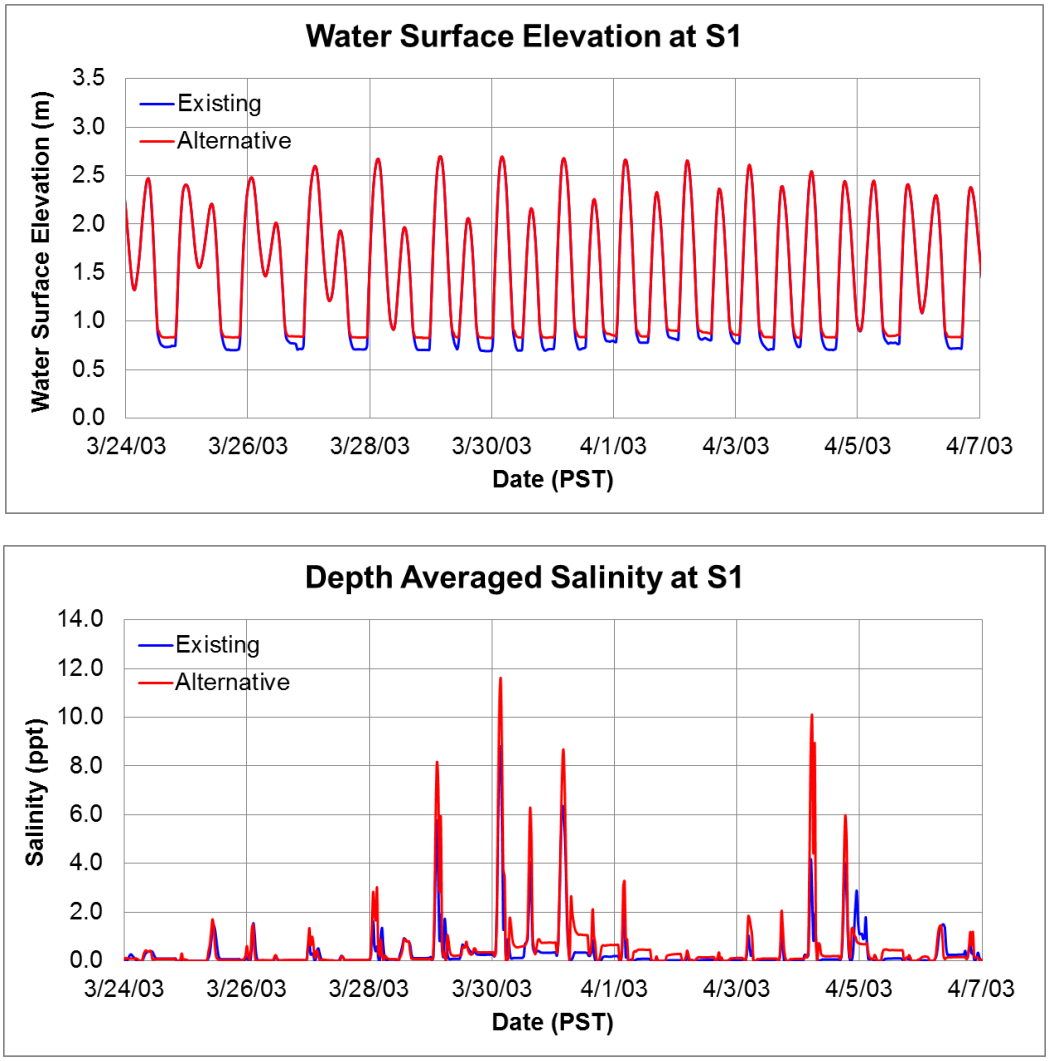

Figure 3.11. Time series of the water level and salinity at Station S1 in the Skagit Bay front.

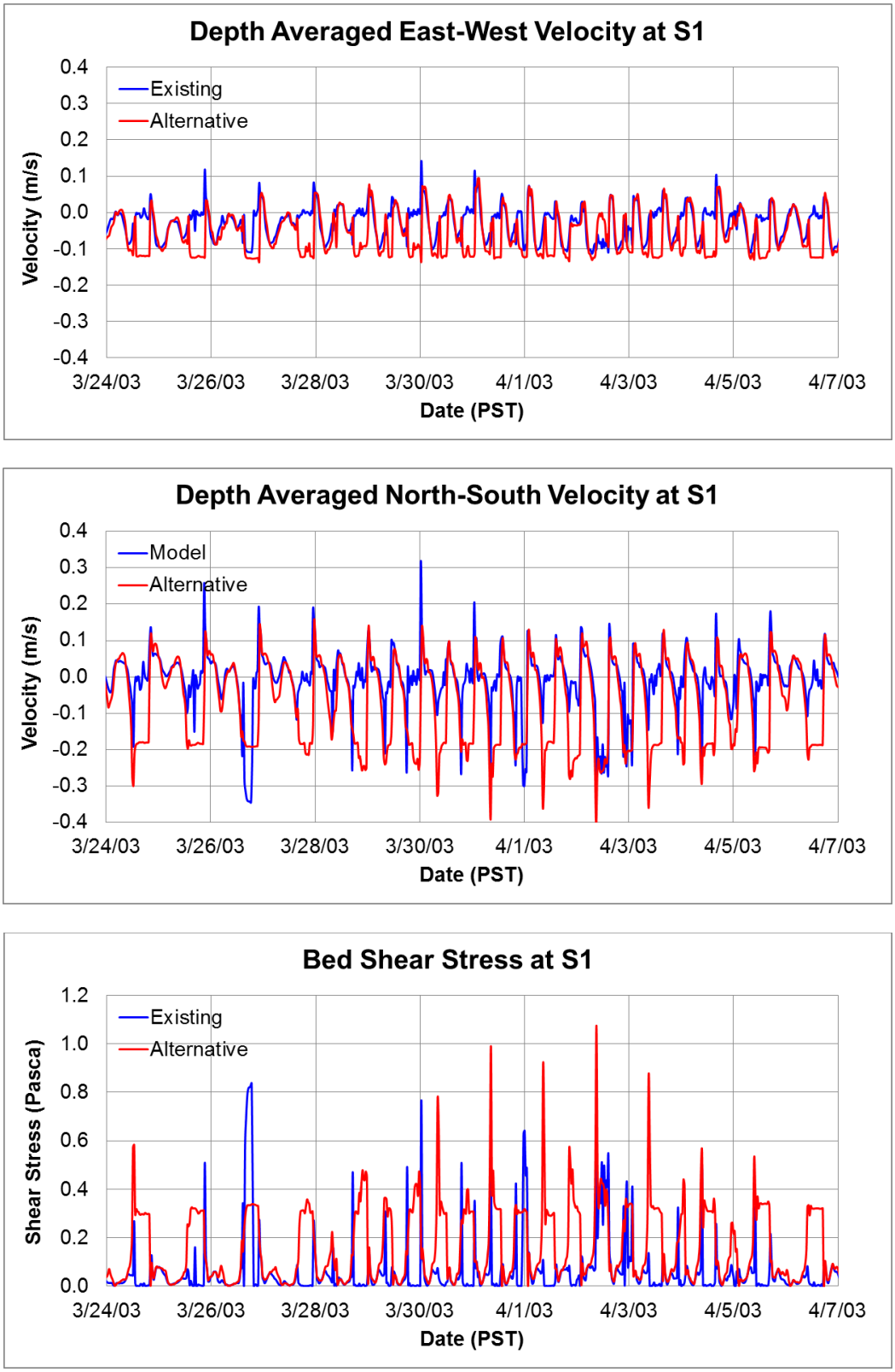

Figure 3.12. Time series of the depth-averaged velocity and bottom shear stress at Station S1 in the Skagit Bay front.

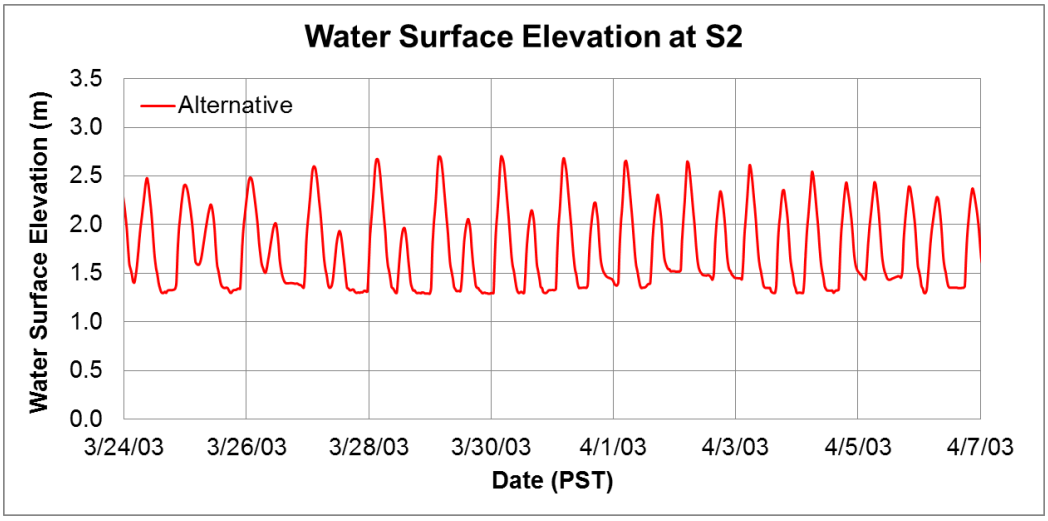

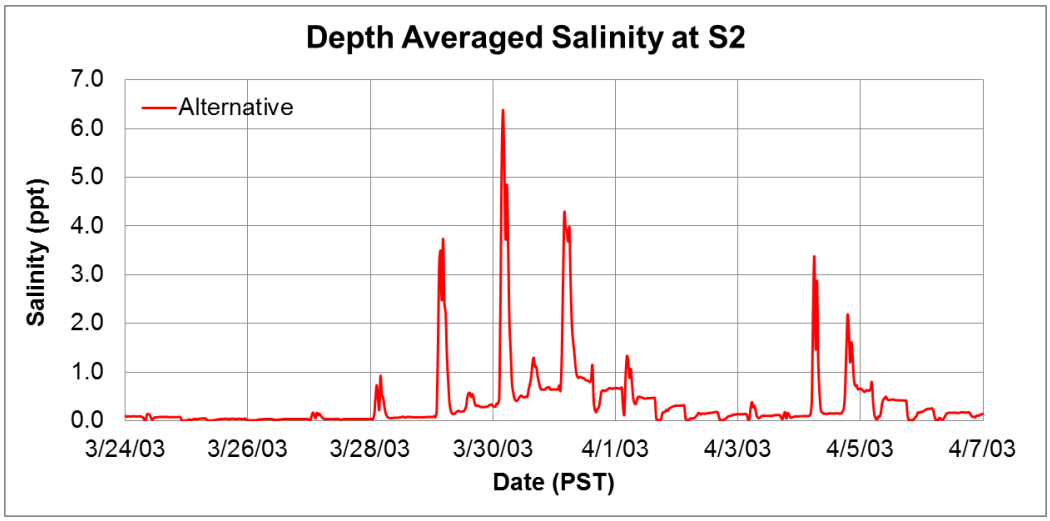

Figure 3.13. Time series of the water level and salinity at Station S2 at the dike opening.

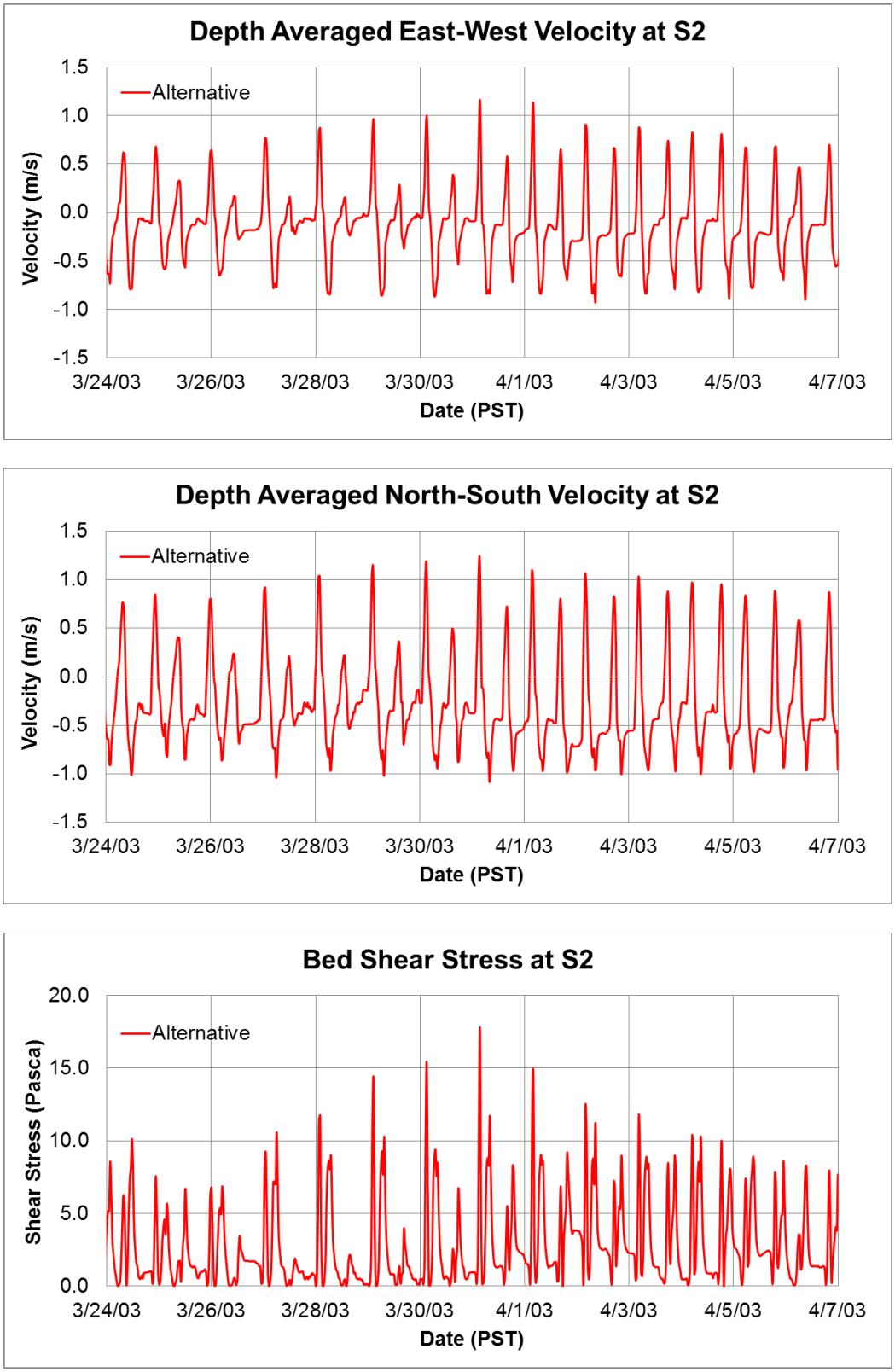

Figure 3.14. Time series of the depth-averaged velocity and bottom shear stress at Station S2 at the dike opening.

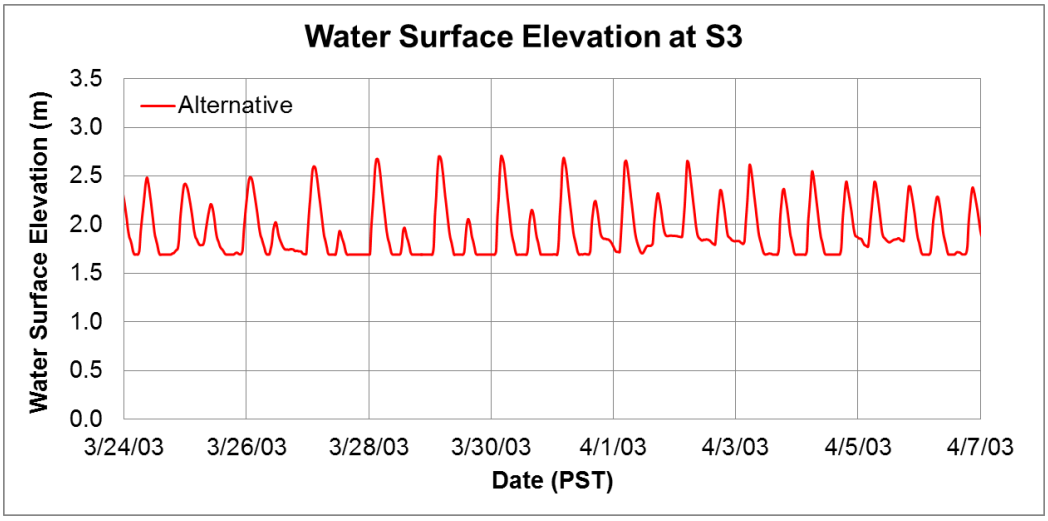

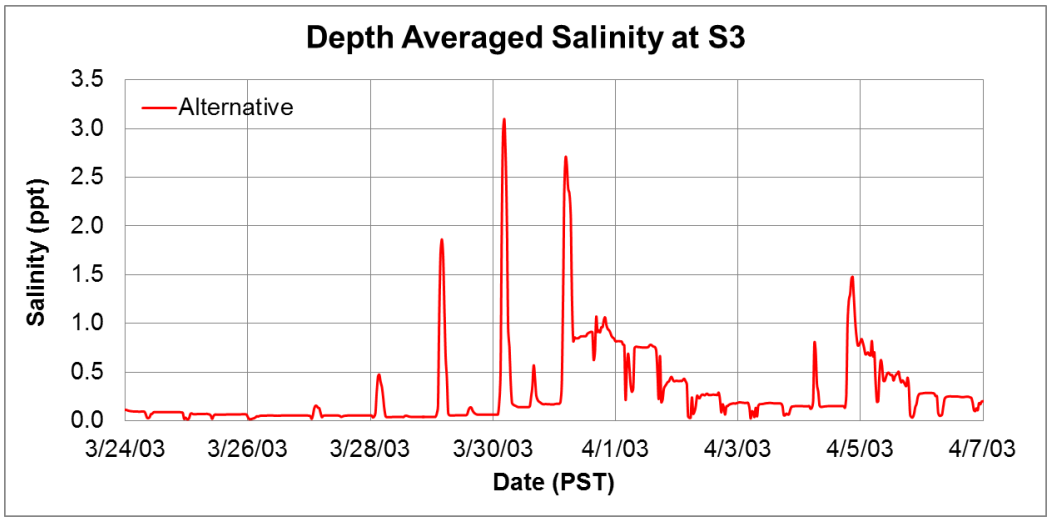

Figure 3.15. Time series of the water level and salinity at Station S3 in No Name Slough.

Figure 3.16. Time series of the depth-averaged velocity and bottom shear stress at Station S3 in No Name Slough.

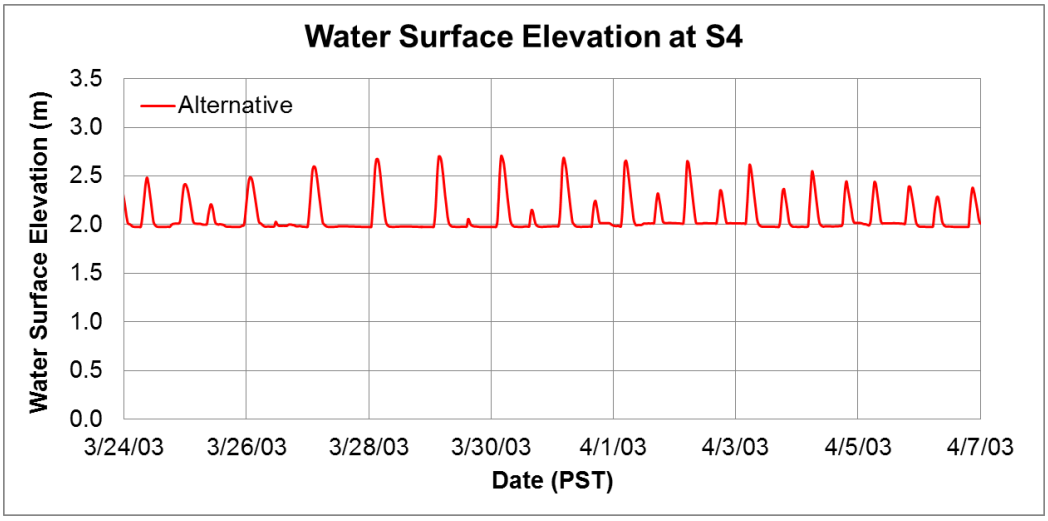

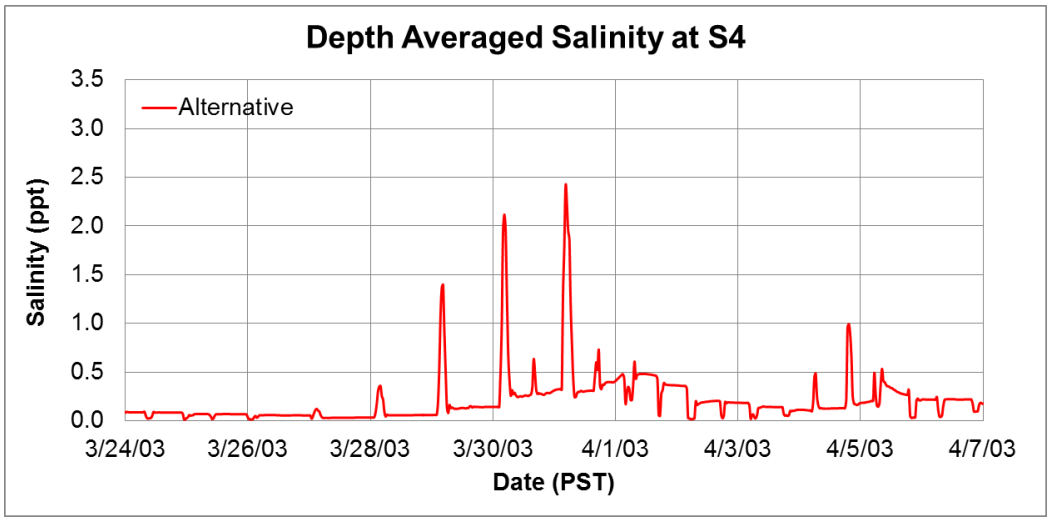

Figure 3.17. Time series of the water level and salinity at Station S4 in the marsh area.

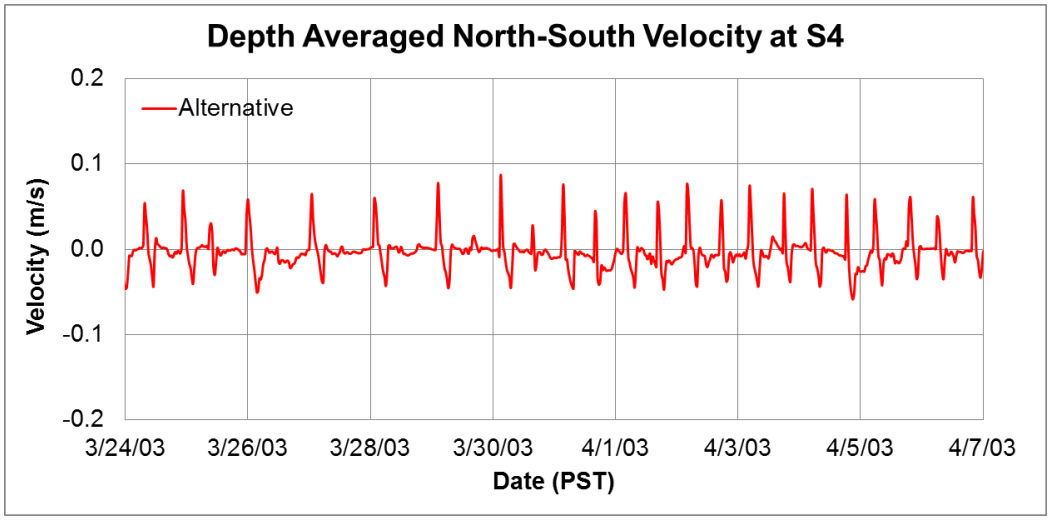

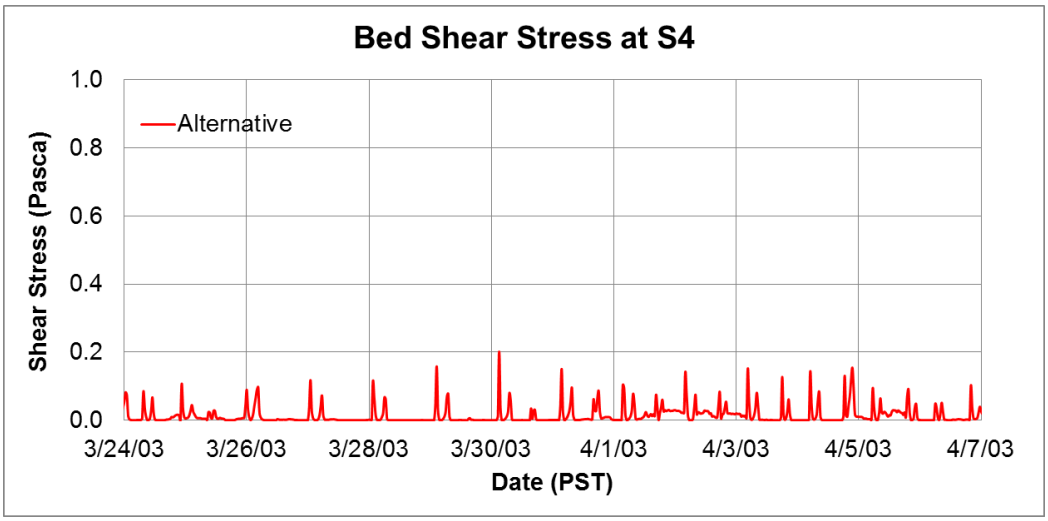

Figure 3.18. Time series of the depth-averaged velocity and bottom shear stress at Station S4 in the marsh area.

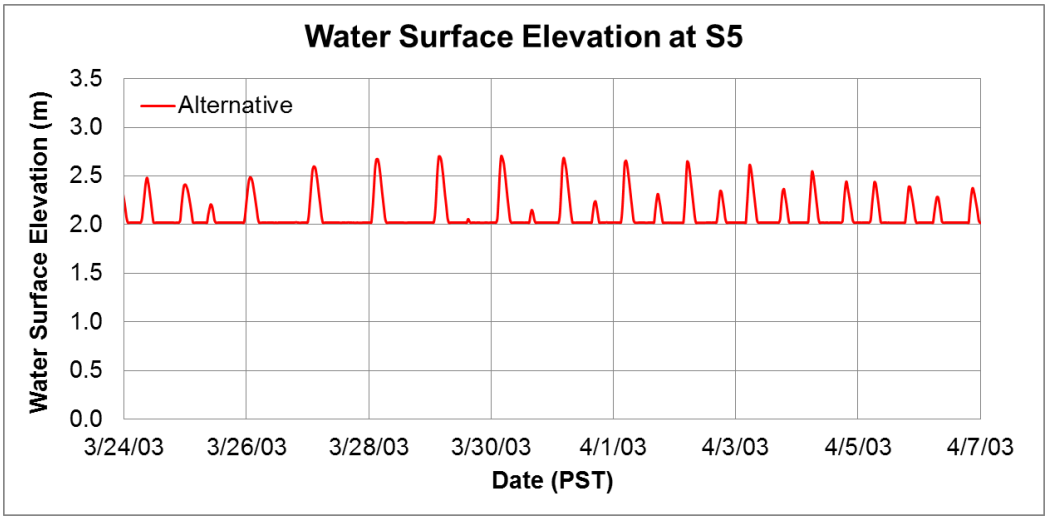

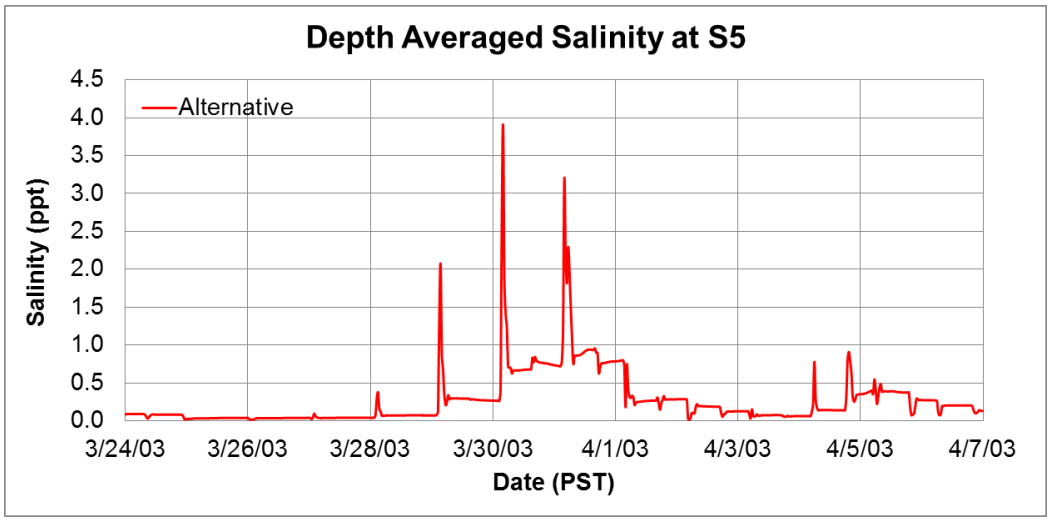

Figure 3.19. Time series of the water level and salinity at Station S5 in Claude O. Davis Slough.

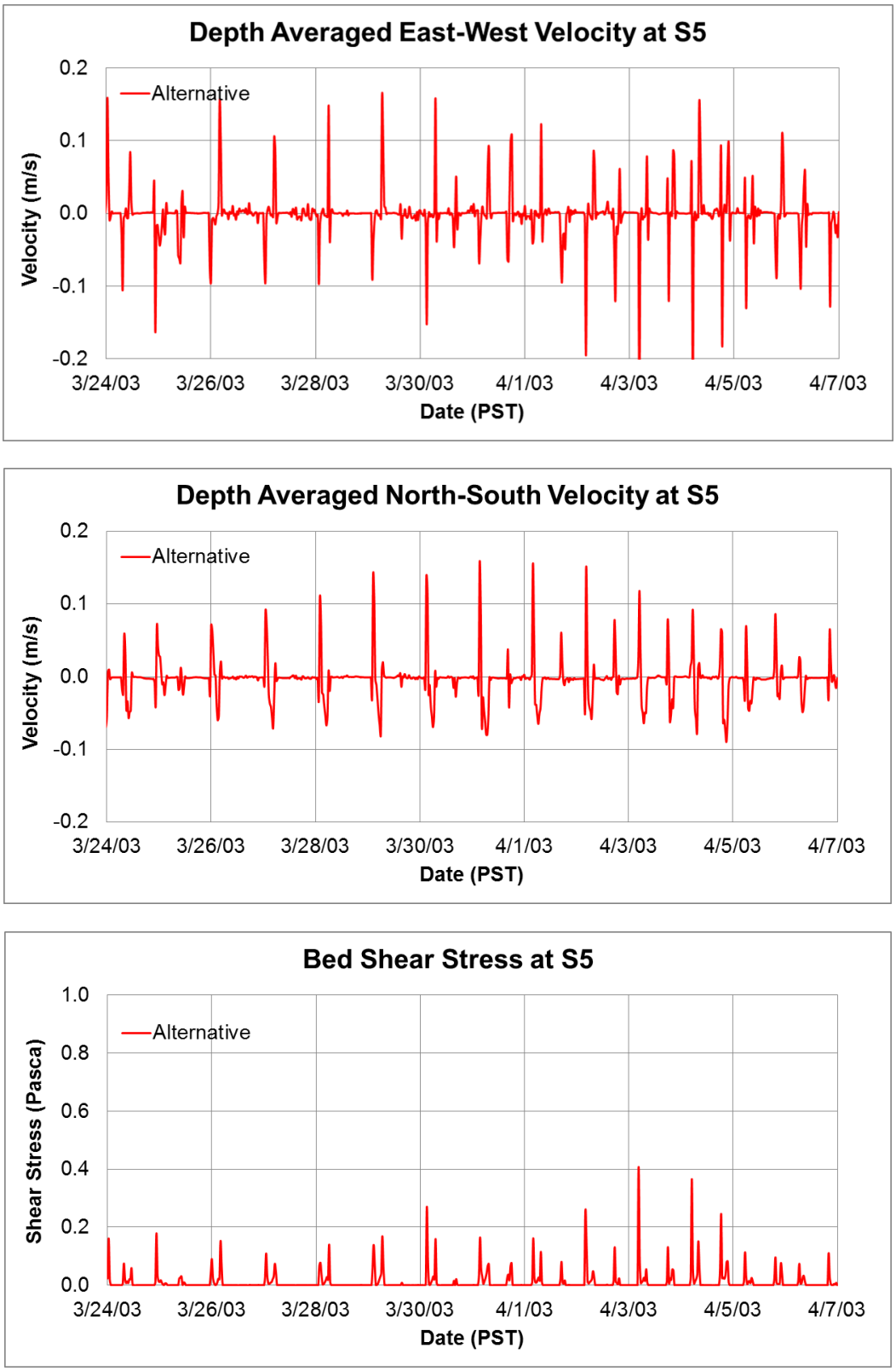

Figure 3.20. Time series of the depth-averaged velocity and bottom shear stress at Station S5 in Claude O. Davis Slough.

Baseline Condition

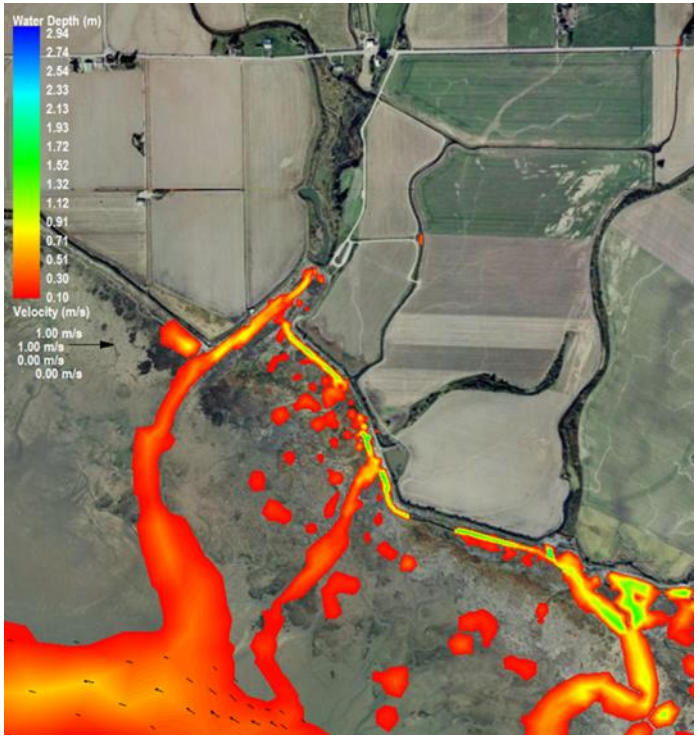

Spur Dike Alternative

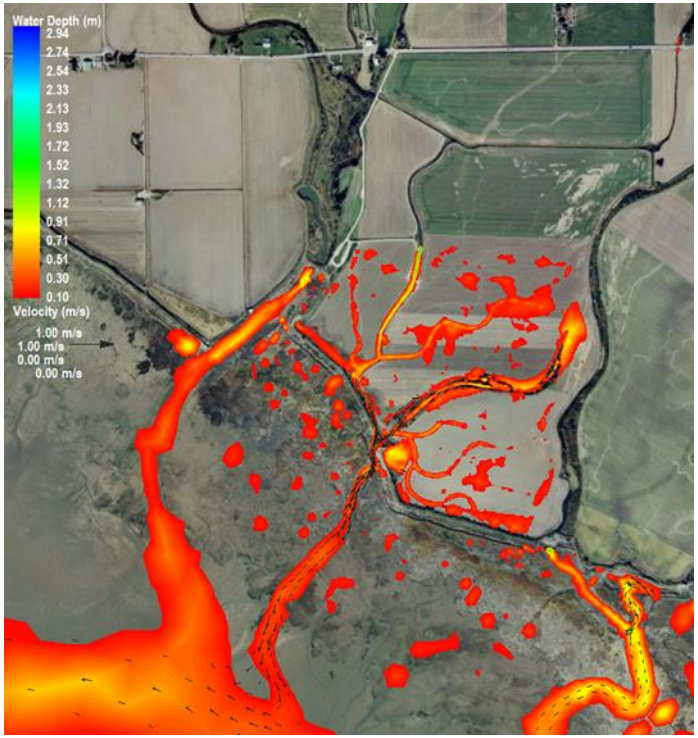

Figure 3.21. Water depth and depth-averaged velocity at low tide (4/13/2003, 8:00 p.m.) for the baseline and spur dike alternative conditions.

Baseline Condition

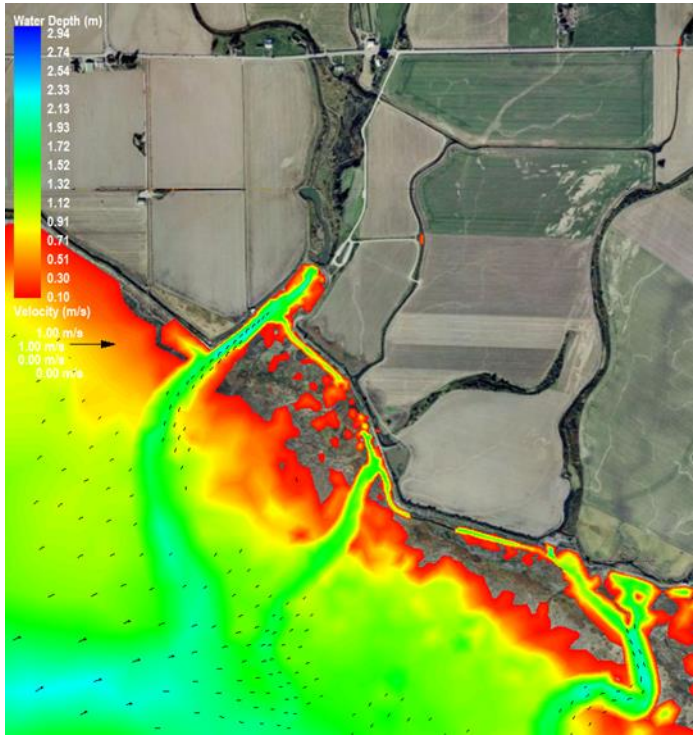

Spur Dike Alternative

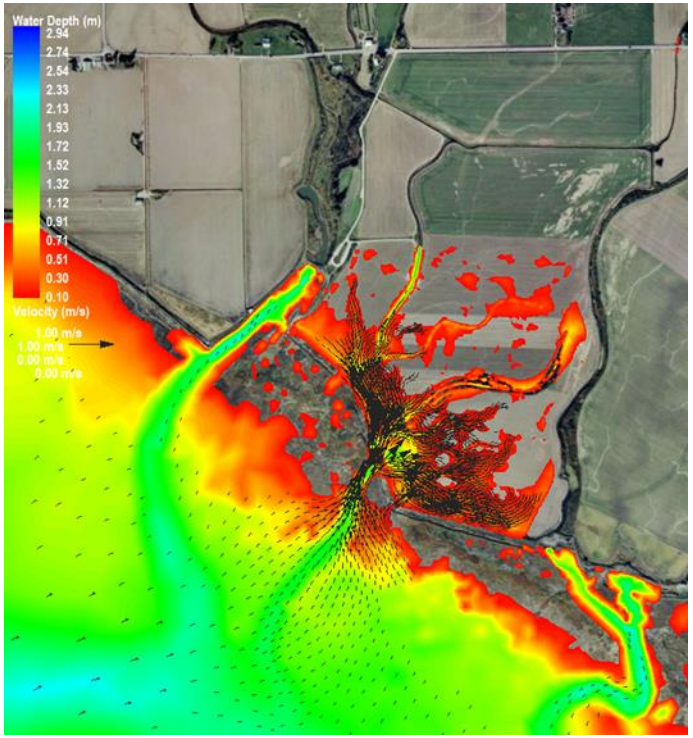

Figure 3.22. Water depth and depth-averaged velocity at flood tide (4/14/2003, 1:30 a.m.) for the baseline and spur dike alternative conditions.

Baseline Condition

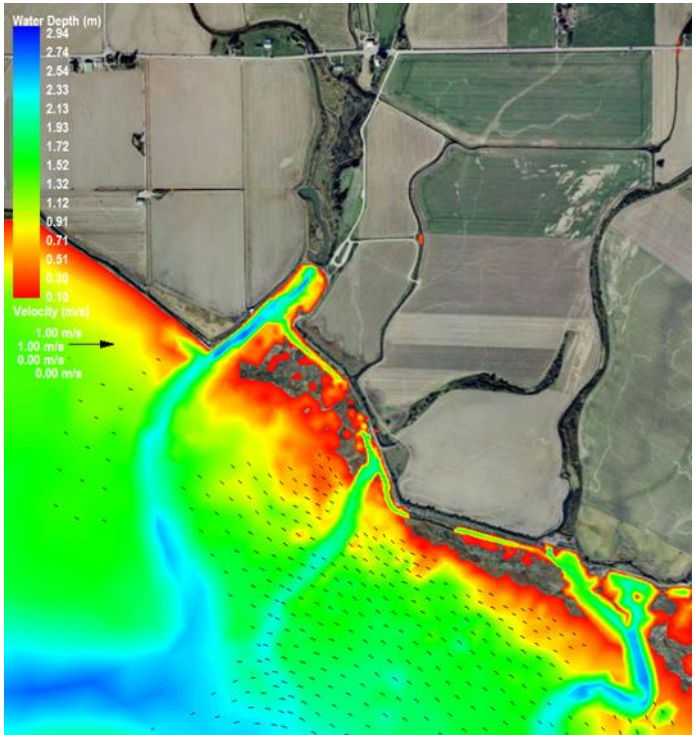

Spur Dike Alternative

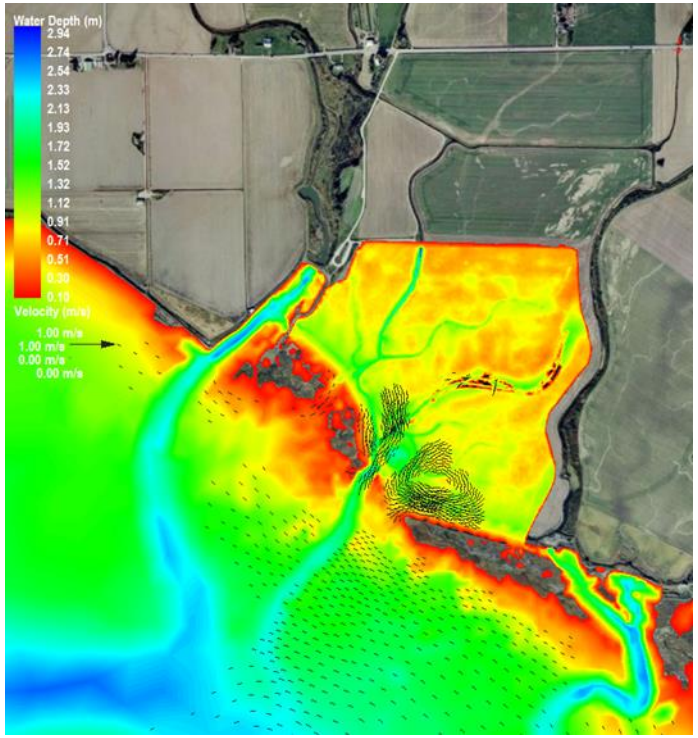

Figure 3.23. Water depth and depth-averaged velocity at high tide (4/14/2003, 3:00 a.m.) for the baseline and spur dike alternative conditions.

Baseline Condition

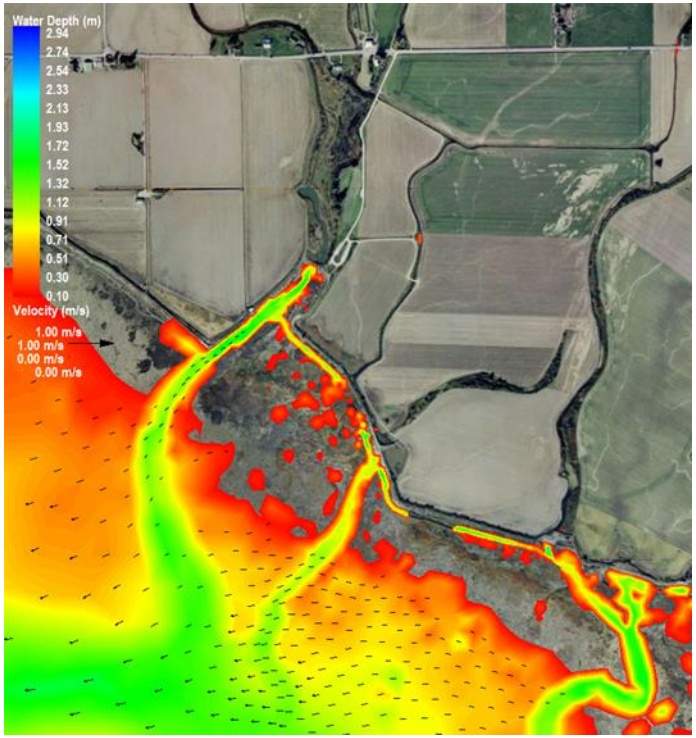

Spur Dike Alternative

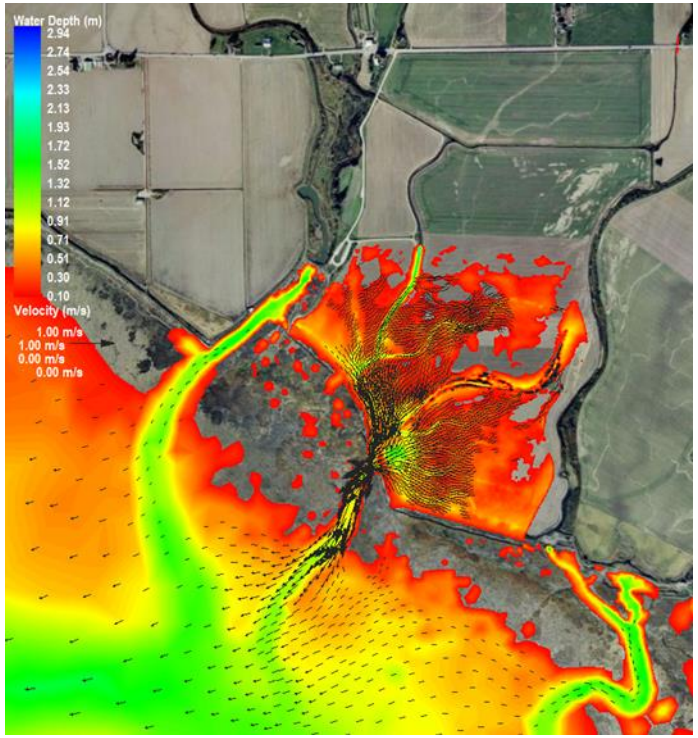

Figure 3.24. Water depth and depth-averaged velocity at ebb tide (4/14/2003, 6:00 a.m.) for the baseline and spur dike alternative conditions.

4.0 Estimate of Maximum Water Level

To further evaluate the risk of flooding or overtopping on the new dike around the restored project site under extreme high tides, storm surges, and future sea level rise conditions, the maximum water level near the project site was estimated and analysis is presented in this section.

4.1 Analysis Approach

An analysis approach that combines numerical model results and observed data was used to estimate the maximum water-surface elevation near the project site. Specifically, water-surface elevation near the project site was determined based on the combination of four components: 1) extreme tides, 2) wave run-up, 3) wind storm surge (local) using the new Skagit Bay hydrodynamic model including the Fir Island Farm restoration site, and 4) long term sea-level rise.

The maximum water level η_{max} is computed as the sum of the following four components:

$$\eta_{max} = \eta_{tide} + \eta_{surge} + \eta_{wave} + \eta_{slr} \tag{4.1}$$

where η_{tide} is the long-term maximum tidal elevation, η_{surge} is the water-surface elevation caused by storm surge, η_{wave} is the wave run-up induced by wind-generated waves, and η_{slr} is the change in water level due to sea-level rise. It is assumed that there is no significant stream flow discharged into the project site because the interior drainage flows in the project site are very small compared to the tidal prism. Calculations of each individual elevation component are described in the following subsections.

4.1.1 Estimate of Extreme Tidal Elevation (η_{tide})

In this study, model simulation was conducted for the period from 3/15/2003 to 4/15/2003, which did not correspond to the extreme high tide conditions. The longest astronomic tidal cycle is about 19 years. Therefore, the extreme tidal elevation was estimated using long-term (19-year) predicted tide data from the XTide database at the Crescent Harbor station, which is located just outside of Skagit Bay. The maximum tidal elevation from the 19-year record (from 1/1/2003 to 1/1/2022) at Crescent Harbor is 3.359 m, which is 0.296 m higher than the maximum tidal elevation of 3.063 m for the period from 3/15/2003 to 4/15/2003. The maximum tidal elevation at Station S2 at the bay front of the project site is 3.066 (see S2 location in Figure 3.9). Assuming such an increase of tidal elevation in Crescent Harbor is linearly proportional to the tidal elevation in the bay front of the project site, then the extreme tidal elevation in the bay front of Fir Island Farm would be η_{tide} = 3.362 m (3.066 m + 0.296 m).

4.1.2 Estimate of 100-Year Storm Surge Height (η_{surge})

Extreme storm events can result in a significant water level surge in the coastal zone. Storm surge is primarily caused by high winds and a low pressure drop on the sea surface. Low pressure at the center of a storm system, such as a hurricane, could have a significant, large-scale effect on the water level along the open coastline. In the Pacific Northwest, we rarely experience cyclonic storms, which have a low pressure at the center and a large pressure gradient. Therefore, water level setup by atmospheric pressure drop in the Fir Island Farm project site was not considered in this study.

The storm surge height was estimated based on wind forcing alone in this study. The 100-year storm wind was estimated based on 66 years of long-term wind record (1948 to 2013) at the National Oceanic and Atmospheric Administration's National Climate Data Center station (72797524255) on Whidbey Island (Figure 2.1). Wind data were recorded at a station height of 14.3 m above mean sea level. To simulate the wind-driven storm surge, wind forcing at a 10-m height should be used in the model. Therefore, wind speed data were adjusted from 14.3 m to the standard 10-m height based on the wind profile power law (Robeson and Shein 1997). The empirical method described by Gupta (1989) was used for the peak wind frequency analysis (Figure 4.1). The relation between peak wind speed and the probability of exceedance can be obtained by a regression-fit to the data:

$$V_{wind} = 29.58\exp(-0.003P) \tag{4.2}$$

where V_{wind} is the peak wind speed corresponding to the percentage of storm occurrence P over a 100-year period. Based on Equation (4.2), the peak wind speed for a 100-year storm event (P =1) was 29.49 m/s. Analysis of wind speed and direction distributions for the entire record period showed that wind directions were primarily from south southwest from April to September and from northwest from October to March (Figure 4.2).

Wind-induced storm surge was simulated using the Skagit Bay hydrodynamic model with spur dike restoration alternative for a 10-day period from 3/16/2003 – 3/26/2003, which corresponds to the spring tide (Figure 2.4). The 100-year storm wind speed of 29.49 m/s blowing from a south-southwest direction (210° clockwise from the north) was specified. This approach would be a conservative estimation of wind-induced surge height at the project site because the maximum wind speed was kept constant for the entire simulation time. Model results showed that the water-surface elevation near the project site may rise about η_{surge} = 0.67 m at high tide during a 100-year storm surge induced by high winds (Figure 4.3).

4.1.3 Estimate of Wave Run-up (η_{wave})

In this study, calculation of significant wave height was based on the Army Corps Engineer (ACE) Shore Protection Manual (1975) using the 100-year peak wind data. For a conservative estimate, it was assumed that the peak wind is blowing directly to the project site and maximum wave height is fully developed. The estimated fetch from the eastern shore of Whidbey Island near the entrance of Penn Cove to the project site is about 20 km. Assuming a shallow water wave condition in Skagit Bay (an average water depth of 3 m), the estimated significant wave height H_b and period T_b are 1.1 m and 4.6 s, respectively, during extreme storm condition with a maximum wind speed of 29.49 m/s (67 mph) based on the forecasting curves of shallow water waves in the U.S. Army Coastal Engineering (ACE) Shore Protection Manual (Figure 3-22 in ACE [1975]).

The wave run-up elevation, which is defined as that super elevation of the mean water level caused by wave action alone, can be calculated based on the formula in the ACE Shore Protection Manual (1975) using the estimated significant wave height and period as the incoming wave condition. During the 100-year storm event and high tide condition, the average water depth in the bay front area near the project site is estimated to be 1.236 m (normal high tide + storm surge + average bed elevation = 3.066+0.67-2.5=1.236). Based on the wave-breaking criteria of H_b/Depth (1.1/1.236=0.89) $\geq$0.78, the incoming wave will break before reaching bay front due to shallow water depth. Under breaking wave conditions, the

kinetic energy of the broken wave would be converted to a quasi-steady potential energy and the wave run-up can be calculated by following formula (Equation (3-49) in ACE [1975]).

$$\eta_{wave} = 0.19\left[1 - 2.82\left(\frac{H_b}{gT_b{}^2}\right)^{1/2}\right]H_b = 0.19\left[1 - 2.82\left(\frac{1.1}{9.8(4.6)^2}\right)^{1/2}\right]1.1 = 0.166\ m \tag{4.3}$$

Therefore, the estimated wave run-up height in the bay front during a 100-year wind storm event is η_{surge} = 0.166 m.

4.1.4 Long-Term Sea Level Rise (η_{slr})

In this study, the effect of relative sea-level rise (SLR) was superimposed on top of the water level at the project site based on values reported from literature review. Various factors, including changes in wind patterns, the gravitational and deformational effects of modern land ice melting, and the vertical land motion, contribute to the sea level rise along the U.S. West Coast. Mote et al. (2008) showed that the very low, medium, and very high estimates of relative SLR in Puget Sound are 0.08 m, 0.15 m, and 0.55 m by 2050 and 0.16 m, 0.34 m, and 1.28 m by 2100, respectively, based on the combined estimates of Intergovernmental Panel on Climate Change (IPCC) global SLR projections and location atmospheric dynamic factors. Mazzotti et al. (2008) estimated that relative SLR at Seattle by 2100 will be 0.34 m with a 90% confidence range of 0.22 m – 0.46 m from a combined tide-gage and global positioning system analysis. Most recently, the U.S. National Academy of Sciences conducted a detailed analysis of the SLR trends along the U.S. West Coast based on IPCC global SLR projections and relevant data and model results, as well as recently published research results (NAS 2012). The vertical land motion projection rate in the Cascadia Subduction Zone was 1.0 mm/yr with a standard deviation of 1.5 mm/yr, where positive rate denotes uplift (NAS 2012; Verdonck 2006). The committee projected that SLR at Seattle contributed by all the factors is η_{slr} = 0.166 m with an uncertainty of ±0.105 m for the year 2050, and η_{slr} = 0.618 m with an uncertainty of ±0.293 m for the year 2100. The relative SLR value of 0.618 m estimated by NAS (2012) is higher than the value given by Mazzotti et al. (2008) but is within the range of those given by Mote et al. (2008). Because the NAS study was a comprehensive study that was based on most recent research results, including the studies by Mazzotti et al. (2008) and Mote et al. (2008), the NAS value of 0.618 ± 0.293 m was used in the maximum water level estimate in this study, as shown in Section 4.2 below.

4.2 Estimate of Maximum Water Level

Based on the estimates of water levels presented in Section 4.1, the maximum water level η_{max} at the Fir Island Farm restoration project site can be estimated using Equation (4.1):

$$\eta_{max} = 3.362 + 0.67 + 0.166 + 0.618 = 4.816 \text{ m (NAVD88)} \tag{4.4}$$

It should be noted that this projection of future maximum water level in the bay front is a conservative estimate because of the underlying assumptions. With the uncertainty of ± 0.293 m in the SLR estimate, the maximum water level for a 100-year extreme event could be as high as 5.109 m (16.76 ft) in the bay front of the Fir Island Farm restoration project site.

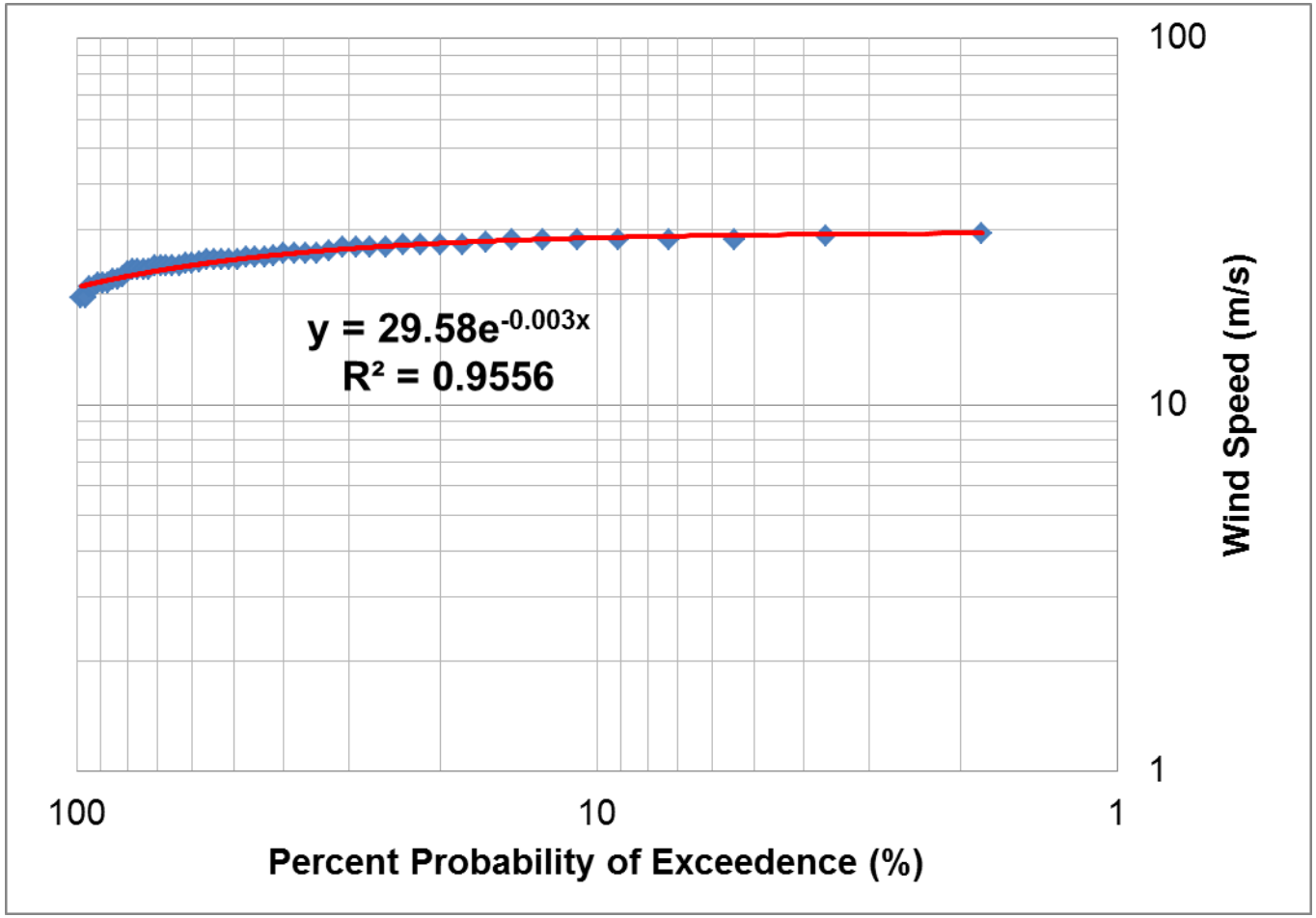

Figure 4.1. Wind frequency curve at NCDC station (72797524255) on Whidbey Island.

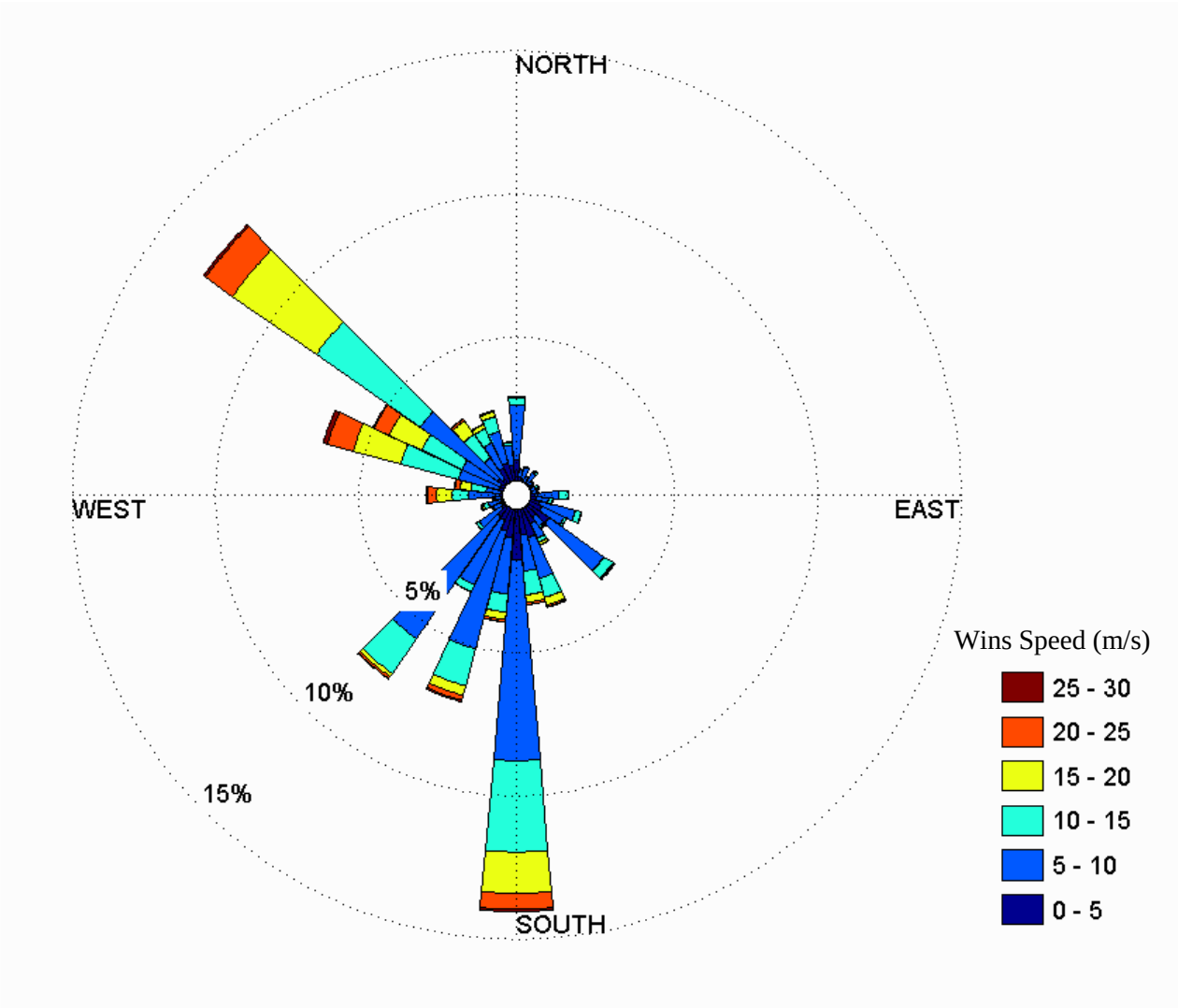

Figure 4.2. Wind rose for the period of 1948−2013 at the NCDC station (72797524255) on Whidbey Island.

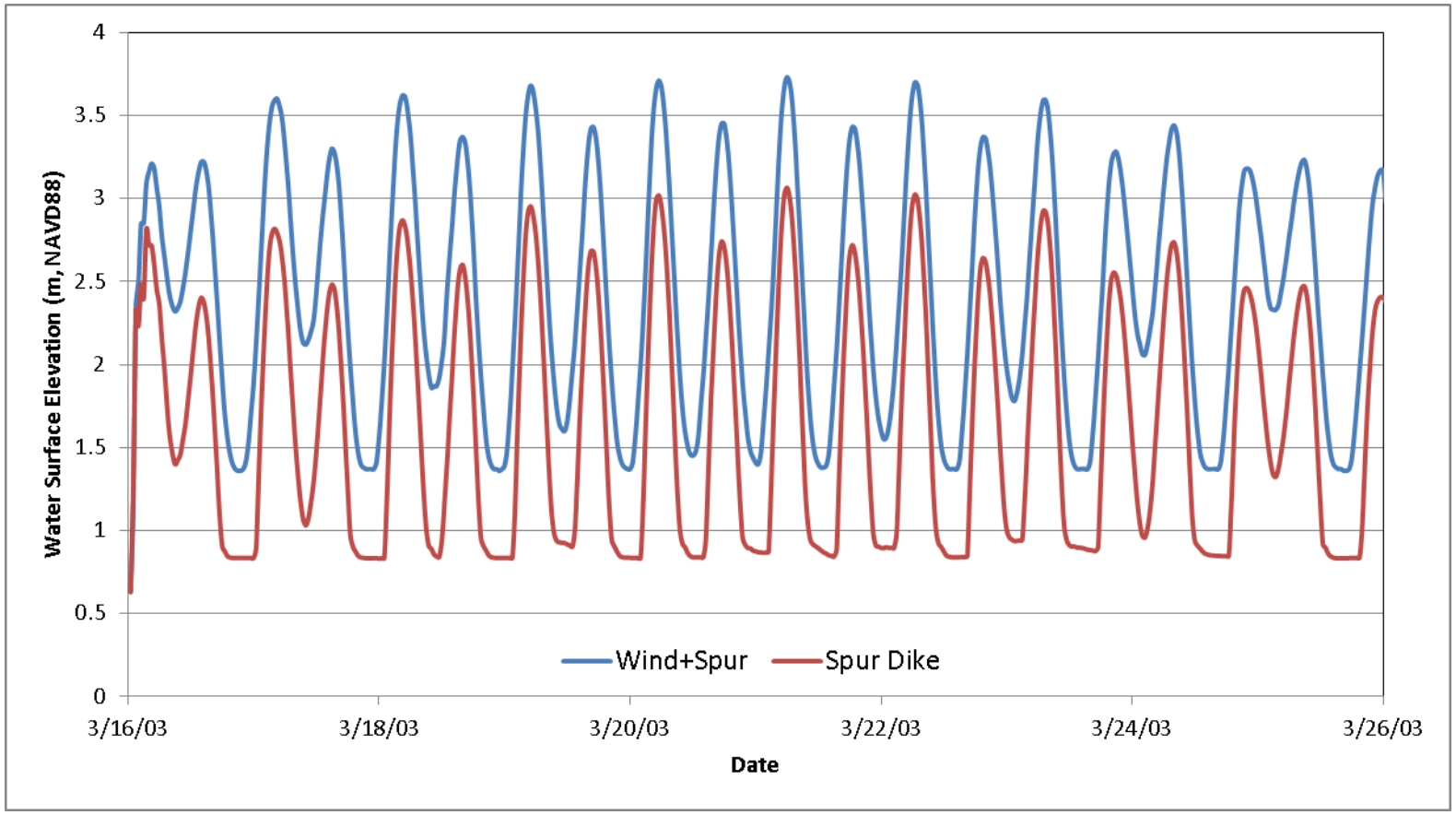

Figure 4.3. Comparison of water-surface elevation at the bay front for the 100-year wind storm and spur dike conditions.

5.0 Conclusions

This report presents the results of the hydrodynamic modeling analysis of the existing condition at the Fir Island Farm restoration site, the restoration conditions (full dike removal and spur dike alternatives) and maximum water-surface elevation near the project site under the condition of an extreme high tide, the 100-year storm event and regional relative sea-level rise.

In conclusion, the model results for the restoration conditions suggest tidal function in the Fir Island Farm project site can be restored after the removal of the bay-front dike. The area downstream from Claude O. Davis Slough will be the primary path for tidal flow. Some initial erosion is expected to occur near the channel openings to the project site. Within the restoration site, tidal velocity and bed shear stress will be generally small. The restoration of tidal marsh in Fir Island Farm may also slightly increase the salinities in the bay-front waters. The spur dike to the east of Brown Slough can effectively block the tidal exchange between Brown Slough and the restoration site.

The maximum water-surface elevation due to the combined effects of an extreme high tide, the 100-year storm event, and regional sea-level rise was estimated based on model simulations, coastal engineering calculation, and literature review. The maximum water level projection for a 100-year return period was 4.816 m (North American Vertical Datum of 1988), which was estimated under the assumptions that the 100-year maximum wind was blowing continuously in the same direction and the storm event would occur at the same time as the extreme high tide. It should be noted that the wind-induced surge was simulated under normal spring tide condition. The empirical method (Equation 4.1) also assumed there is no interaction among wind relative sea level rise, wind storm surge and extreme high tide. To account for the nonlinear interaction between these forcing mechanisms and their effects on maximum water level near the project site, additional model simulations driven by all the extreme forcing functions at the same time are necessary.

6.0 References

ACE (U.S. Army Coastal Engineering Research Center). 1975. *Shore Protection Manual*. Volume 1. Available at: (http://archive.org/details/shoreprotectionm01coas).

Breithaupt S, Z Yang, and T Wang. 2011. "Hydrodynamic Modeling Analysis of Fir Island Farm Restoration – Preferred Alternative." Technical Memorandum PNWD-4306, provided to Shannon & Wilson, Inc. by Pacific Northwest National Laboratory, Richland, Washington.

Chen C, H Liu, and RC Beardsley. 2003. "An unstructured, finite-volume, three-dimensional, primitive equation ocean model: application to coastal ocean and estuaries." *Journal of Atmospheric Oceanic Technology* 20:159–186.

Gupta R.S. 2007 Hydrology and Hydraulic Systems, Waveland Press, Inc., Long Grove, IL.

Mazzotti S. C Jones, and RE Thomson. 2008. "Relative and absolute sea level rise in western Canada and northwestern United States from a combined tide gauge-GPS analysis." *Journal of Geophysical Research* 113, C11019, doi:10.1029/2008JC004835.

Mote PW, A Petersen, S Reeder, H Shipman, and LC Whitely Binder. 2008. *Sea Level Rise in the Coastal Waters of Washington State*. Climate Impacts Group, University of Washington and the Washington Department of Ecology, Seattle, Washington,

NAS (National Academy of Sciences). 2012. *Sea-Level Rise for the Coasts of California, Oregon, and Washington: Past, Present and Future*. Committee on Sea Level Rise in California, Oregon, and Washington. Board on Earth Sciences and Resources and Ocean Studies Board. The National Academies Press, Washington, D.C.

Robeson SM and KA Shein. 1997. "Spatial coherence and decay of wind speed and power in the north-central United States." *Physical Geography* 18:479−495.

Verdonck D. 2006. "Contemporary vertical crustal deformation in Cascadia." *Technophysics* 417:221–230.

Yang Z and T Wang. 2011. "Hydrodynamic Modeling Analysis of Fir Island Farm Restoration – Baseline Condition." Technical Memorandum, PNWD-SA-9379, provided to Shannon & Wilson, Inc. by Pacific Northwest National Laboratory, Richland, Washington.

Yang Z and T Khangaonkar. 2009. "Modeling Tidal Circulation and Stratification in Skagit River Estuary Using an Unstructured Grid Ocean Model." *Ocean Modelling* 28:34−49. doi: 10.1016/j.ocemod.2008.07.004.

Acknowledgement

This study was funded by Washington State Department of Fish and Wildlife through a subcontract with Shannon & Wilson, Inc.